nature COMMUNICATIONS

OPEN

ARTICLE

Received 14 Nov 2011 | Accepted 11 Jan 2012 | Published 14 Feb 2012

DOI: 10.1038/ncomms1677

Interferon-γ-producing immature myeloid cells confer protection against severe invasive group A *Streptococcus* infections

Takayuki Matsumura[1], Manabu Ato[1], Tadayoshi Ikebe[2], Makoto Ohnishi[2], Haruo Watanabe[2] & Kazuo Kobayashi[1]

Cytokine-activated neutrophils are known to be essential for protection against group A *Streptococcus* infections. However, during severe invasive group A *Streptococcus* infections that are accompanied by neutropenia, it remains unclear which factors are protective against such infections, and which cell population is the source of them. Here we show that mice infected with severe invasive group A *Streptococcus* isolates, but not with non-invasive group A *Streptococcus* isolates, exhibit high concentrations of plasma interferon-γ during the early stage of infection. Interferon-γ is necessary to protect mice, and is produced by a novel population of granulocyte–macrophage colony-stimulating factor-dependent immature myeloid cells with ring-shaped nuclei. These interferon-γ-producing immature myeloid cells express monocyte and granulocyte markers, and also produce nitric oxide. The adoptive transfer of interferon-γ-producing immature myeloid cells ameliorates infection in wild-type and interferon-γ-deficient mice. Our results indicate that interferon-γ-producing immature myeloid cells have a protective role during the early stage of severe invasive group A *Streptococcus* infections.

[1] Department of Immunology, National Institute of Infectious Diseases, 1-23-1 Toyama, Shinjuku-ku, Tokyo 162-8640, Japan. [2] Department of Bacteriology I, National Institute of Infectious Diseases, 1-23-1 Toyama, Shinjuku-ku, Tokyo 162-8640, Japan. Correspondence and requests for materials should be addressed to M.A. (email: ato@nih.go.jp).

© 2012 Macmillan Publishers Limited. All rights reserved.

Streptococcus pyogenes (group A *Streptococcus*; GAS) is one of the most common human pathogens. It causes a wide variety of infections, ranging from uncomplicated pharyngitis and skin infections to severe and even life-threatening manifestations such as streptococcal toxic shock syndrome (STSS) and necrotizing fasciitis. The mortality rates for STSS and necrotizing fasciitis are high (30–70%), even following prompt antibiotic therapy and debridement[1–4].

It is widely believed that myeloid cells including polymorphonuclear leukocytes (PMNs) have a central role in survival from GAS infections, and interferon (IFN)-γ is essential to full activation and proper function of PMNs. Notably, IFN-γ at the infection site is thought to be critical for protection; however, its increased systemic levels seem to be detrimental to survival after GAS infections[5]. Therefore, the appropriate regulation of cytokine-producing cells may be critical for survival and host defense against severe invasive GAS infections.

Myeloid cells with ring-shaped nuclei (ring cells) are present in the peripheral blood of patients with myeloproliferative diseases, but only rarely in healthy control subjects[6,7]. Ring cells are usually referred to as PMNs. However, not only Gr-1^{high} PMN-like ring cells, but also Gr-1^{low} mononuclear cell-like ring cells are present in the bone marrow, peripheral blood, and inflammatory infiltrates of mice[8]. Morphologically, a part of myeloid-derived suppressor cells (MDSCs) has ring-shaped nuclei[9,10]. MDSCs are potent suppressors of T-cell immunity, and their presence is associated with a poor clinical outcome in cancer. They are divided into 2 subtypes according to morphology and surface markers: Ly-6G$^-$ Ly-6C^{high} monocytic MDSCs and Ly-6G$^+$ Ly-6C^{low} granulocytic MDSCs[11,12]. Recent studies have demonstrated the considerable suppressive potential of MDSCs on T-cell immunity in autoimmune diseases, and also in chronic infections with intracellular pathogens, such as *Salmonella typhimurium*, *Candida albicans*, *Trypanosoma cruzi*, and *Toxoplasma gondii*[13]. However, the biological functions of ring cells in infectious diseases, and also the relationship between ring cells and MDSCs, remain largely unknown.

In the present study, IFN-γ-producing immature myeloid cells with ring-shaped nuclei (γIMCs), which originated from bone marrow precursor-like cells (BMPCs), are shown to be functionally and phenotypically distinct from MDSCs. We demonstrate that γIMCs have a protective role against severe invasive GAS infections, and possibly compensate for neutropenia.

Results

Role of IFN-γ in severe invasive GAS infections. To clarify the types of cytokines involved in severe invasive GAS infections, we first investigated the dynamics of cytokines in severe invasive and non-invasive GAS infections. As a model of disseminated infection in normally sterile sites, we intraperitonially (i.p.) infected GAS-susceptible C3H/HeN mice[14–17] with either severe invasive (*emm3* genotype *rgg* gene-mutated STSS strain, NIH34) or non-invasive (*emm3* genotype non-STSS (pharyngitis) strain, K33) GAS clinical isolates[18], and measured the levels of plasma cytokines. We detected no significant amount of plasma cytokines within 24 h of infection. By contrast, in mice infected with severe invasive GAS isolates, but not with non-invasive GAS isolates, we detected high levels of plasma IFN-γ; moreover, the levels increased rapidly at 48 h post-infection (Fig. 1a). Other cytokines, such as IL-1α, IL-1β, IL-4, IL-5, IL-12 p70 and IL-17, were scarcely detected in the plasma of mice infected with either severe invasive or non-invasive isolates. By contrast, in mice infected with severe invasive GAS isolates, the levels of IL-2, IL-10, and TNF increased transiently at 36 h post-infection.

Further, we evaluated whether IFN-γ is the host factor contributing to protection against severe invasive GAS infections, or to deterioration of STSS through an augmented inflammatory process. We i.p. administered mice with an anti-mouse IFN-γ neutralizing mAb (clone R4-6A2), on the day of infection with severe invasive GAS isolates. At 72 h post-infection, all of the mice administered with the IFN-γ neutralizing mAb died. By contrast, 50% of the mice treated with rat IgG as a control survived (Fig. 1b). These results are consistent with those of a previous study[5], in which mice treated with a different IFN-γ neutralizing mAb (clone XMG1.2) and IFN-γ knockout (*Ifng*$^{-/-}$) mice were more susceptible to lethal skin infection with the M-nontypeable GAS strain 64/14 than were control IgG-administered mice and wild-type mice, respectively. Thus, IFN-γ may act as a host defense factor against severe invasive GAS infections.

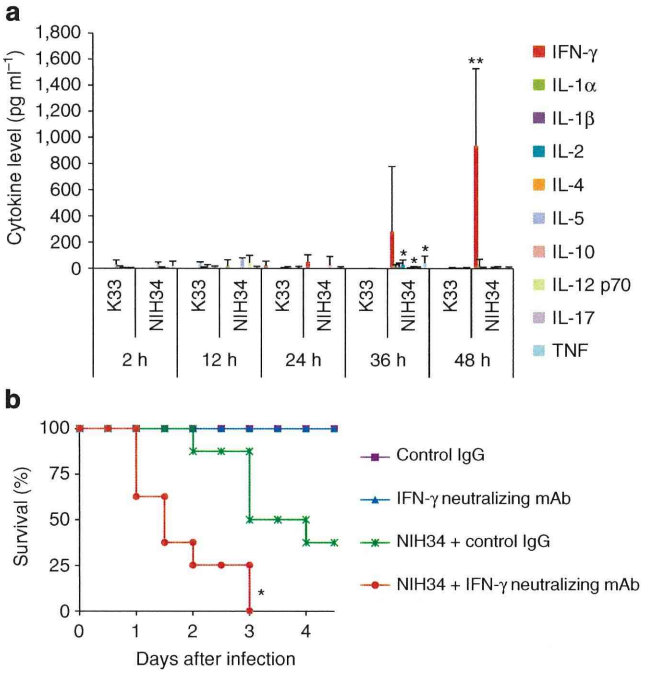

Figure 1 | IFN-γ is a host defense factor in mice infected with severe invasive GAS isolates. (**a**) C3H/HeN mice were i.p. inoculated with *S. pyogenes* (*emm3* genotype) clinical isolates (non-STSS, K33; STSS, NIH34; 3.0×10^7 CFU per mouse), and plasma cytokine levels were determined by FlowCytomix. Data are expressed as mean±s.d. for at least 2 independent experiments, using a total of 6–10 mice for each group. The differences compared with K33-infected mice were statistically significant (*P<0.05, **P<0.01) as determined by Student's t-test. (**b**) C3H/HeN mice were i.p. inoculated with NIH34 (3.0×10^7 CFU per mouse) in the presence of an IFN-γ neutralizing mAb (clone R4-6A2) (1 mg per mouse) or control rat IgG (1 mg per mouse). Survival was observed for 4 days post-infection. Mortality differences compared with infected mice in the presence of control IgG were statistically significant (*P<0.05), as determined by a log-rank test. Survival curves were generated from two independent experiments, using a total of eight mice for each group.

A source of IFN-γ in severe invasive GAS infections. It is widely believed that T cells are a main source of IFN-γ in severe invasive GAS infections[19–21]. To identify the IFN-γ-producing cell types in mice infected with severe invasive GAS isolates, we used an *in vivo* intracellular cytokine synthesis (ICS) assay[22,23] to assess splenic IFN-γ production at 48 h post-infection. Unexpectedly, we revealed that Gr-1$^+$ CD11b$^+$ cells (but not TCR-β$^+$ TCR-γ/δ$^+$, CD4$^+$, or CD8$^+$ T cells, DX5$^+$ NK/NKT cells, or CD11c$^+$ MHC-II$^+$ dendritic cells) were a source of splenic IFN-γ in superantigen-insensitive C57BL/6 mice[24,25], and also in C3H/HeN mice (Fig. 2a and b). These Gr-1$^+$ cells appeared in the spleen on day 1 post-infection, subsequently increased in number, and were the major source of IFN-γ

© 2012 Macmillan Publishers Limited. All rights reserved.

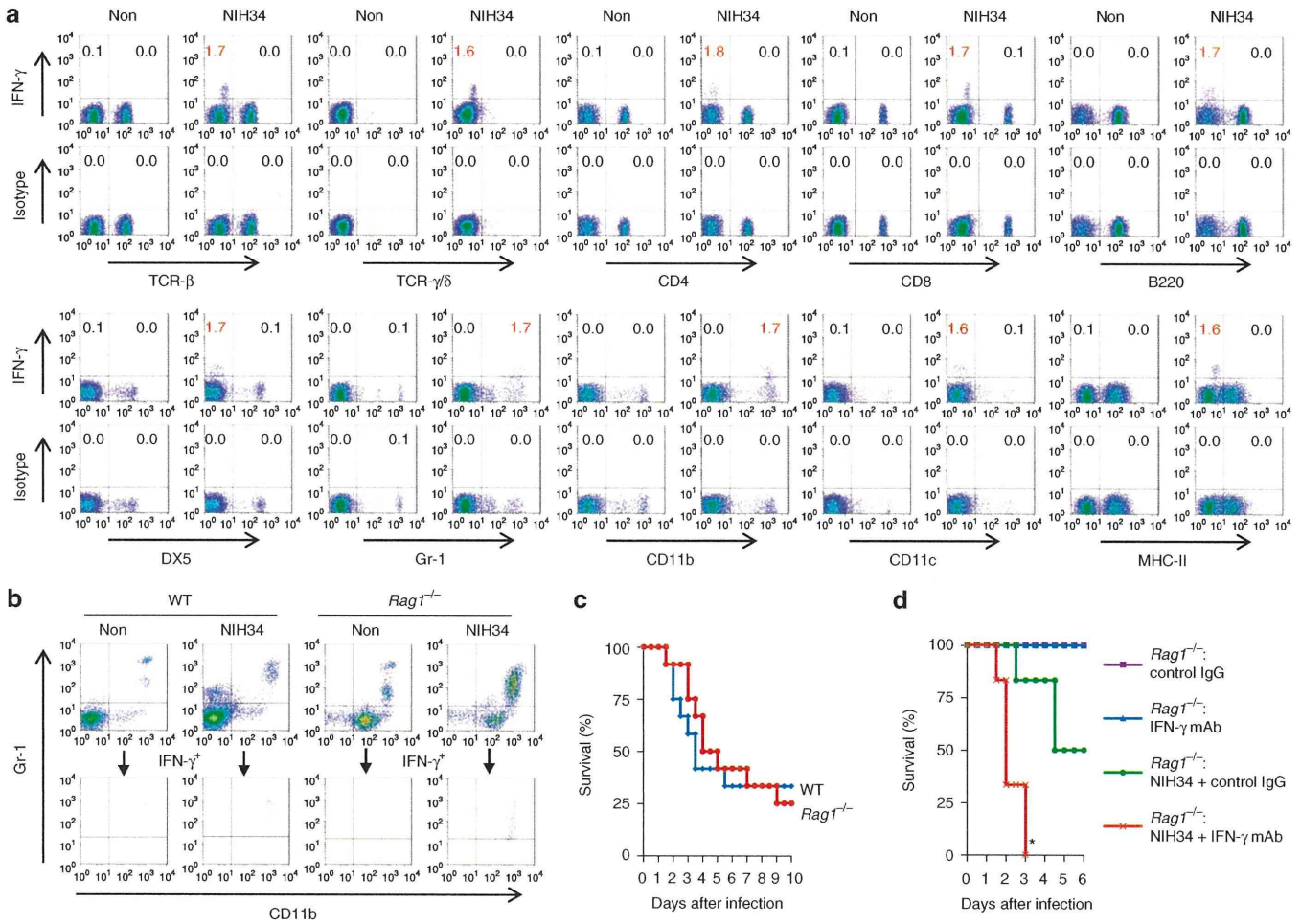

Figure 2 | CD11b$^+$ Gr-1$^+$ cells are the source of IFN-γ in severe invasive GAS infections. (**a**,**b**) C3H/HeN mice (**a**), C57BL per six mice (WT) (**b**), and *Rag1*$^{-/-}$ mice (**b**) with or without i.p. infection of NIH34 (3.0×10^7 CFU per mouse) for 42 h were i.v. injected with monensin. Six hours later, the mice were sacrificed and their splenocytes were immediately stained for the indicated markers, and analysed by ICS assay. (**a**) The numbers (%) in the plots represent the proportion of IFN-γ$^+$ subsets to total splenocytes. (**b**) Lower panels show the cells gated on the IFN-γ$^+$ population. Data are representative of three independent experiments. (**c**,**d**) WT and *Rag1*$^{-/-}$ mice were i.p. inoculated with NIH34 (3.0×10^7 CFU per mouse) in the absence (**c**) or presence (**d**) of an IFN-γ neutralizing mAb (clone R4-6A2) or control rat IgG (1 mg per mouse) as in Fig. 1b. Survival (in days) was observed as indicated. Survival curves were generated from 2 independent experiments, using a total of 12 mice for each group. (**d**) Mortality differences compared with infected mice in the presence of control IgG were statistically significant (*$P < 0.05$) as determined by a log-rank test.

throughout infection (Supplementary Fig. S1). By contrast, TCR-β$^+$ T cells and DX5$^+$ or NK1.1$^+$ NK cells, which are regarded as the sources of IFN-γ in GAS infections[15–17], produced small amounts of IFN-γ during the late stage (days 3–5 post-infection) of severe invasive GAS infections in C3H/HeN mice, but not in C57BL/6 mice. Notably, the accumulation of Gr-1$^+$ cells led to the clearance of infection from the spleen. Additionally, the administration of monensin, which blocks intracellular cytokine transport, did not induce spontaneous splenic production of IFN-γ (Fig. 2a and b; Supplementary Fig. S1).

To exclude the involvement of T cells in protection against severe invasive GAS infections, we investigated IFN-γ production in C57BL/6.RAG1 knockout (*Rag1*$^{-/-}$) mice, which have no mature B and T cells[26]. The ICS assay revealed that the cellular source of IFN-γ during severe invasive GAS infections was Gr-1$^+$ CD11b$^+$ cells in *Rag1*$^{-/-}$ mice, and also in C57BL/6 wild-type (WT) mice (Fig. 2b). We further examined the mortality of *Rag1*$^{-/-}$ mice during severe invasive GAS infections. We observed no significant difference in mortality between *Rag1*$^{-/-}$ and WT mice infected with severe invasive GAS isolates (Fig. 2c). Furthermore, similar to C3H/HeN mice (Fig. 1b), IFN-γ neutralizing mAb (clone R4-6A2)-treated *Rag1*$^{-/-}$ mice were more susceptible to severe invasive GAS infections than were control IgG-administered *Rag1*$^{-/-}$ mice (Fig. 2d). Our results indicate that mature B and T cells do not affect the mortality of infected mice, and that T cells have no protective effect during the early stage of severe invasive GAS infections.

Characterization of the early source of IFN-γ. Anti-Gr-1 mAb detects Ly-6C$^+$ monocytes and Ly-6G$^+$ PMNs. Therefore, to determine which subset of Gr-1$^+$ CD11b$^+$ cells is responsible for IFN-γ production during severe invasive GAS infections, we investigated the surface phenotype of IFN-γ-producing cells isolated from the spleens of mice at 48 h post-infection. The ICS assay revealed that IFN-γ-producing cells had the phenotype of monocytes (F4/80^{low} CX3CR1$^+$) and PMNs (Ly-6G$^+$ Ly-6C^{low}) (Fig. 3). Additionally, they expressed no lymphoid (CD27, IL-7Rα) or granulocyte-lineage (CCR3, Siglec-F, c-Kit, IL-5Rα (H7)) markers, but exhibited particular profiles of CCR2$^-$ CD31$^+$ CD34$^-$ CD38$^+$ CD44^{high} CD49d$^+$ CD62L$^+$ CD69$^+$ IL-5Rα (T21)^{high} Siglec-H$^-$ (Fig. 3; Supplementary Table S1). In this model, the most prominent GAS infection was present in the kidney[18,27]. In accordance with the bacterial burden in the peritoneal cavity, spleen and kidney, a higher proportion

© 2012 Macmillan Publishers Limited. All rights reserved.

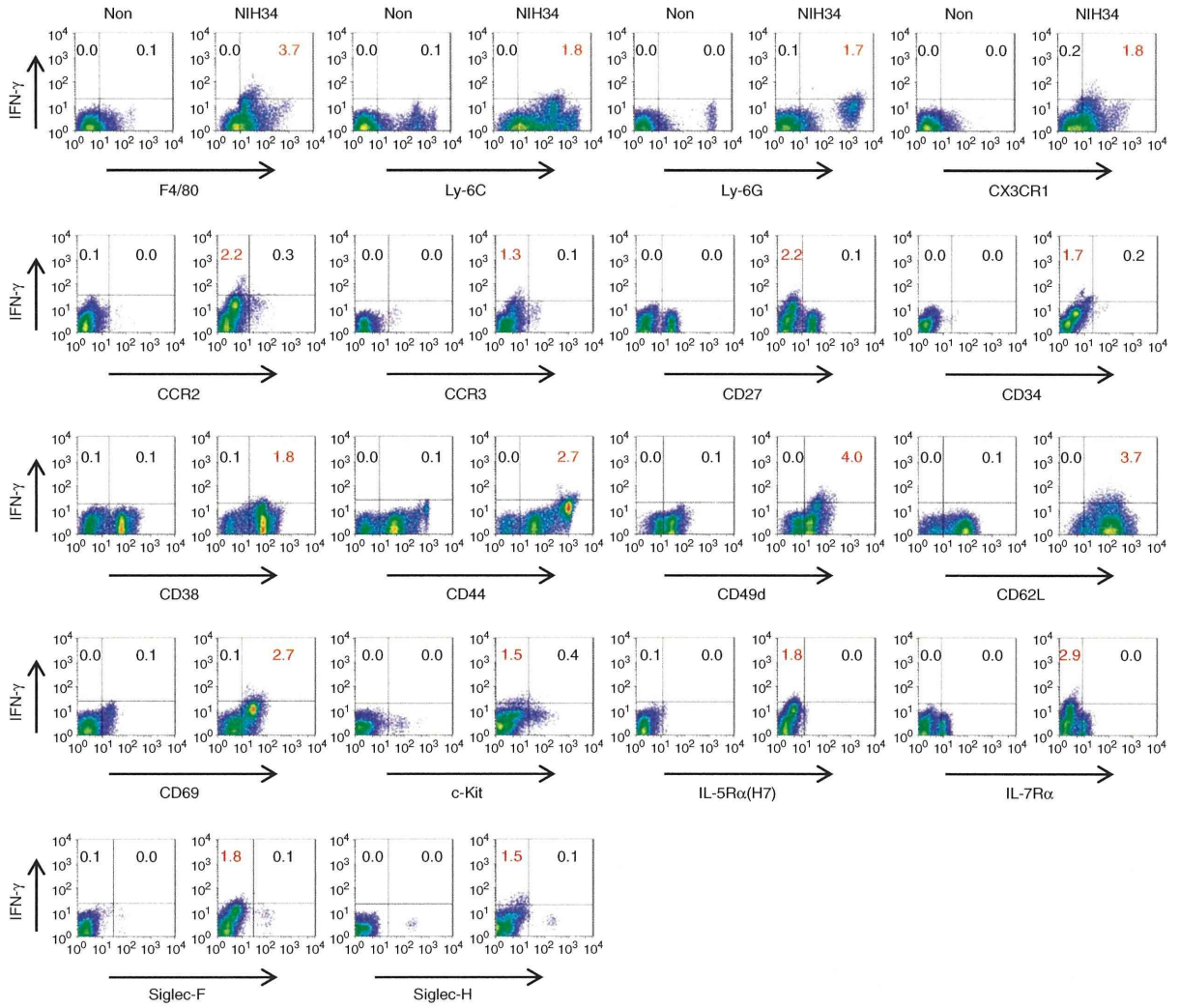

Figure 3 | IFN-γ-producing cells exhibit monocyte and PMN phenotypes in severe invasive GAS infections. C3H/HeN mice with or without i.p. infection of NIH34 (3.0×10^7 CFU per mouse) for 42 h were i.v. injected with monensin. Six hours later, the mice were killed and their splenocytes were immediately stained for the indicated markers, and analysed by the ICS assay. The numbers (%) in the plots represent the proportion of IFN-γ$^+$ subsets to total splenocytes. These data are representative of three independent experiments.

of IFN-γ-producing cells accumulated in the kidney of C3H/HeN mice, and also C57BL/6 mice i.p. infected with NIH34 (Supplementary Fig. S2). By contrast, lower proportion of IFN-γ-producing cells existed at the sites of infection. A skin-infection model yielded similar results (Supplementary Fig. S2). Furthermore, IFN-γ-producing cells were detected in the spleens from mice infected with various STSS strains[18,27] (Supplementary Fig. S3). These cells were also detected in the peripheral blood and (in particularly high frequency) the bone marrow from NIH34-infected mice (Fig. 4a–d; Supplementary Fig. S4). Interestingly, Siglec-F$^+$ eosinophils (Eos) stained with IL-5Rα (H7) and IL-5Rα (T21), whereas IFN-γ-producing cells stained well with T21, but not with H7 (Fig. 4e), suggesting that IFN-γ-producing cells were phenotypically distinct from Eos. IFN-γ-producing cells were also phenotypically distinct from Ly-6C^{low} CD31$^-$ PMNs (Fig. 4d). Moreover, the number and proportion of PMNs were markedly reduced in the spleen, peripheral blood, and bone marrow at 48 h post-infection (Fig. 4d and f), as reported in human STSS cases[28].

Immature myeloid cells as an early source of IFN-γ. The IFN-γ-producing cells expressed the phenotypic markers of monocytes/macrophages (F4/80 and CX3CR1) and PMNs (Ly-6G). Therefore, we sorted CD11b$^+$ CD11c$^-$ F4/80^{low} Ly-6G$^+$ cells from the spleens of infected mice and morphologically analysed them with May-Grünwald-Giemsa staining. The IFN-γ-producing CD11b$^+$ CD11c$^-$ F4/80^{low} Ly-6G$^+$ splenocytes were IMCs, but not monocytes/macrophages or PMNs. These IFN-γ-producing IMCs were large cells containing ring-shaped, non-segmented nuclei, with a coarse chromatin pattern[6–8] (Fig. 5a and b). The sorted cells were contaminated with a small number of PMNs; however, immunohistochemical analyses showed that IMCs, but not PMNs, were the source of IFN-γ (Fig. 5c). The cells with ring-shaped nuclei were also observed in the peritoneum, kidney, and spleen from i.p. infection model, and in the skin from subcutaneous (s.c.) infection model, whereas such cells were not observed in the spleen and kidney from non-infected or non-invasive K33 strain-infected mice (Fig. 5d and e). To determine whether IFN-γ-producing IMCs (γIMCs) are committed to the granulocyte or monocyte lineage, we cultured sorted CD11b$^+$ CD11c$^-$ F4/80^{low} Ly-6G$^+$ γIMCs *in vitro*, in the presence of G-CSF, M-CSF, GM-CSF or IL-5. We observed that G-CSF, M-CSF and IL-5 failed to promote differentiation and survival (Fig. 5f). By contrast, in the presence of GM-CSF, differentiated γIMCs increased their expression of CD11c, F4/80, DX5 and Siglec-F (Fig. 5g) with the polymorphonuclear phenotype (Fig. 5h). Such granulocyte-like cells showed

© 2012 Macmillan Publishers Limited. All rights reserved.

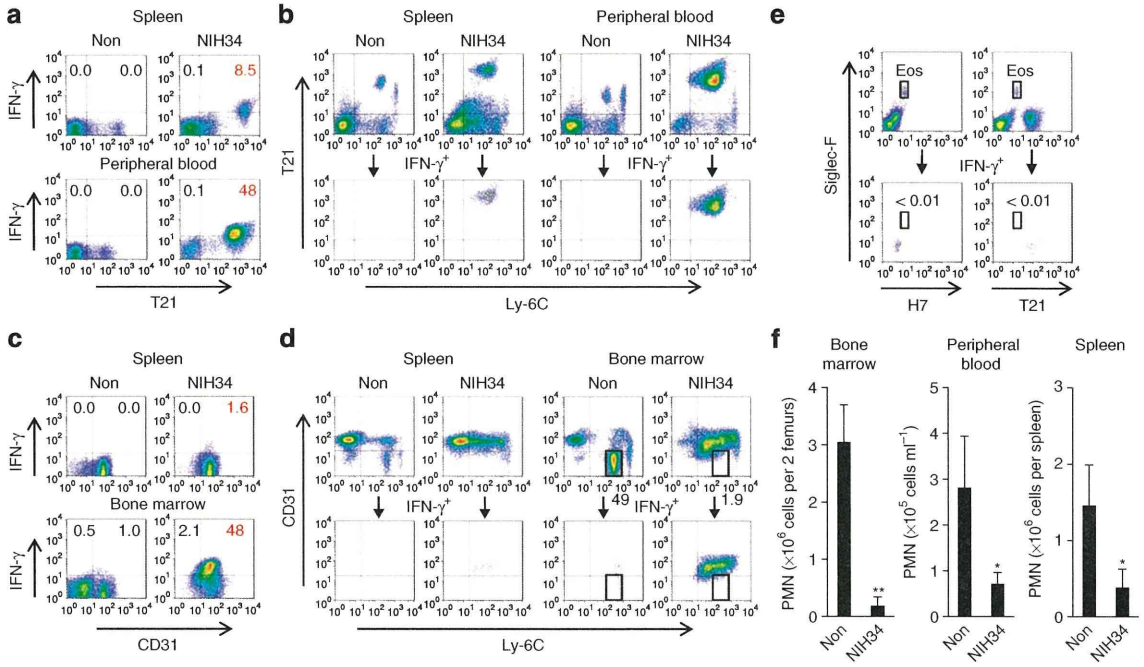

Figure 4 | IFN-γ-producing cells are detected in the peripheral blood and the bone marrow of GAS-infected mice. (**a**–**d**) Non-infected C3H/HeN mice or (**a**–**e**) mice i.p. infected with NIH34 (3.0×10^7 CFU per mouse) for 42 h were i.v. injected with monensin. Six hours later, the mice were killed and their splenocytes (**a**–**e**), peripheral blood cells (**a**,**b**), and bone marrow cells (**c**,**d**) were immediately stained for the indicated markers, and analysed by ICS assay. (**a**,**c**) The numbers (%) in the plots represent the proportion of IFN-γ$^+$ subsets to total cells. (**b**,**d**,**e**) Lower panels show the cells gated on the IFN-γ$^+$ population. (**d**,**e**) Rectangle gates in the plot represent mature granulocytes (**d**) and Eos (**e**). The numbers (%) in the plots represent the proportion of mature granulocytes (**d**) or IFN-γ$^+$ Eos (**e**) to total cells. Data are representative of three independent experiments. (**f**) The numbers of PMNs in the bone marrow, peripheral blood, and spleen from non-infected or NIH34-infected mice at 48 h. Data are expressed as mean±s.d. ($n=3$). The differences compared with non-infected mice were statistically significant (*$P<0.05$, **$P<0.01$) as determined by Student's *t*-test.

reduced ability to produce IFN-γ (Fig. 5i), and were phenotypically different from c-Kit^{low} H7$^+$ Siglec-F$^+$ bone marrow-derived Eos and CCR3$^+$ H7$^+$ Siglec-F$^+$ splenic Eos[29]; (Supplementary Fig. S5). These results suggest that γIMCs are committed to the granulocyte lineage, but do not exist in the steady state, and produce IFN-γ during a specific stage of differentiation.

Nitric oxide (NO) is considered to be a main mechanism for controlling some infective agents. Myeloid cells are able to release NO in response to IFN-γ[30–33]; moreover, IFN-γ and NO-producing myeloid cells have been described in cancer[34]. Therefore, we investigated the ability of γIMCs to produce NO in response to GAS. When stimulated by autocrine and/or paracrine IFN-γ, γIMCs (but not than PMNs and granulocyte-like cells differentiated from γIMCs using GM-CSF) were able to produce NO, because their NO production was significantly blocked in the presence of IFN-γ neutralizing mAb (Fig. 5j).

Differentiation of precursor-like cells into γIMCs. Bone marrow contains the highest proportion of γIMCs (Fig. 4c and d). Therefore, we attempted to identify the precursors of γIMCs in the bone marrow of mice infected with severe invasive GAS isolates. Interestingly, analysis of the surface molecules revealed 2 distinct subsets of IFN-γ-producing cells (Fig. 6a): a minor and a major subset. The minor subset constituted 6.9±3.2% of IFN-γ-producing bone marrow cells (Fig. 6b), and comprised CD11b$^+$ CD11c$^-$ F4/80^{low} Ly-6G$^+$ large cells (Supplementary Fig. S6), containing ring-shaped nuclei (BM-γIMCs) (Fig. 6c). On the basis of morphology and surface phenotype, these cells corresponded to splenic γIMCs (Sp-γIMCs) (Fig. 5a and b). Neither isolated BM-γIMCs nor Sp-γIMCs proliferated in the presence of GM-CSF (Figs 5f and 6d). These cells differed from metamyelocytes and immature neutrophils in non-infected bone marrow (Fig. 6c). The major subset of IFN-γ-producing cells comprised CD11b$^+$ CD11c^{low} F4/80$^+$ Ly-6G^{low} precursor-like cells (BMPCs) (Fig. 6b; Supplementary Fig. S6), which constituted 74.8±13.7% of IFN-γ-producing cells (Fig. 6b). This subset consisted of ~10% monocyte-like ring cells and immature myeloid cells (Fig. 6c), which are phenotypically different from CD11b$^-$ Ly-6G$^-$ cells such as granulocyte–monocyte progenitors, common myeloid progenitors, and myelolymphoid progenitors[35]. In the presence of GM-CSF, isolated BMPCs proliferated (Fig. 6d) and differentiated into BM-γIMCs (Fig. 6c and e). Moreover, after 2 extra days of incubation with GM-CSF, differentiated BM-γIMCs increased their expression of CD11c, F4/80, DX5 and Siglec-F (Fig. 6f). The polymorphonuclear and cell surface phenotype (Supplementary Fig. S6) was similar to that of Sp-γIMCs cultured with GM-CSF (Fig. 5g and h). The differentiation of BMPCs into BM-γIMCs was totally blocked in the presence of IFN-γ neutralizing mAb; by contrast, this cytokine was dispensable for differentiation into granulocyte-like cells (Supplementary Fig. S6). These results are in accordance with the absence of Ly-6G$^+$ γIMCs in the spleen of GAS-infected C57BL6.*Ifng*$^{-/-}$ mice (Supplementary Fig. S7). The expression level of Ly-6G in PMNs was similar for WT and *Ifng*$^{-/-}$ mice (Supplementary Fig. S7). As with γIMCs and γIMC-differentiated granulocyte-like cells (Fig. 5i), the cells differentiated from BMPCs, after 2 extra days of incubation with GM-CSF, retained the ability to release IFN-γ in response to GAS; however, subsequent differentiation by GM-CSF reduced the ability to produce IFN-γ (Fig. 6g). A few IFN-γ-producing cells in non-infected mice were recognized in the same fraction as the BMPCs (Fig. 6a), and, therefore, it is possible that BMPCs exist in the naïve bone marrow. Our results suggest that IFN-γ-producing BMPCs are the precursors of γIMCs, and that their differentiation is dependent on autocrine and/or paracrine pathways involving

© 2012 Macmillan Publishers Limited. All rights reserved.

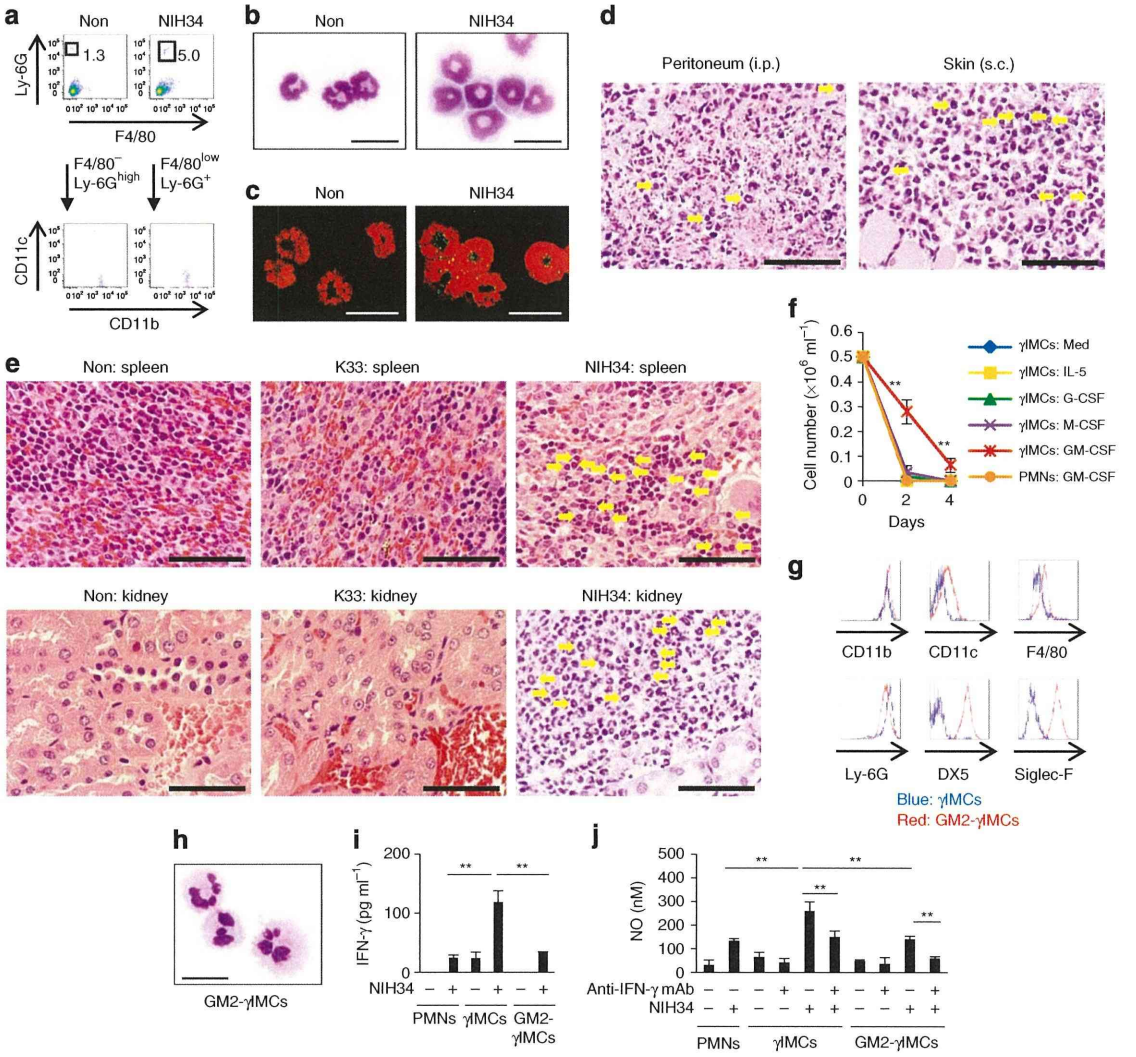

Figure 5 | γIMCs are the source of IFN-γ in severe invasive GAS infections. (**a**) CD11b$^+$ CD11c$^-$ F4/80$^-$ Ly-6G^{high} PMNs in splenocytes from non-infected C3H/HeN mice, or CD11b$^+$ CD11c$^-$ F4/80^{low} Ly-6G$^+$ γIMCs in splenocytes from mice infected with NIH34, were isolated by FACS. (**b**,**c**) Cytospin preparations of each sorted cell type were visualized with May-Grünwald-Giemsa staining (**b**), whereas intracellular IFN-γ (green, IFN-γ; red, nuclei) was visualized with a confocal laser microscopy (**c**). Scale bars, 20 μm. (**d**,**e**) Paraffin-embedded sections of peritoneum, from mice i.p. infected with NIH34 and skin from mice subcutaneously (s.c.) infected with NIH34 for 48 h (**d**), and of spleen and kidney from mice i.p. infected with or without K33 or NIH34 for 48 h, (**e**) were visualized with hematoxylin and eosin staining. The yellow arrows indicate the cells with ring-shaped nuclei. Scale bars, 100 μm. (**f**) Sorted IMCs were cultured with control medium (Med), G-CSF (50 ng ml^{-1}), M-CSF (10 ng ml^{-1}), GM-CSF (10 ng ml^{-1}), or IL-5 (10 ng ml^{-1}) for 2–4 days, and their absolute numbers were counted on the indicated days. Data are expressed as the average (mean ± s.d.) of triplicate wells ($n = 3$). The differences compared with Med were statistically significant (**$P < 0.01$) as determined by Student's t-test. (**g**) γIMCs (blue line) and GM-CSF (2 days)-cultured γIMCs (GM2-γIMCs: red line) were stained for the indicated markers. Data are representative of three independent experiments. (**h**) Cytospin preparations of GM2-γIMCs were visualized with May-Grünwald-Giemsa staining. Scale bars, 20 μm. (**i**,**j**) γIMCs and GM2-γIMCs were cultured with erythromycin-treated NIH34 (MOI 100) in the presence of control rat IgG or an IFN-γ neutralizing mAb (clone R4-6A2) for 24 h. The levels of IFN-γ (**i**) and NO_2^- (**j**) in the culture supernatants were measured by ELISA and Griess reagent system, respectively. The average (mean ± s.d.) of triplicate wells is shown. Statistical significance (**$P < 0.01$) was determined by ANOVA.

IFN-γ. Notably, the BMPC-derived unclassified granulocyte-lineage, such as γIMCs (but not immature PMNs), seems to appear during severe invasive GAS infections.

Distinction between γIMCs and MDSCs. MDSCs are composed of F4/80$^-$ or F4/80^{low} granulocytic MDSCs with ring-shaped nuclei, and F4/80$^+$ monocytic MDSCs[10,11]. They can produce IFN-γ[13]. Furthermore, granulocytic/monocytic MDSCs differentiate into CD11c$^+$ F4/80$^+$ Gr-1$^+$ cells[12], as do γIMCs (Fig. 5g). To identify the relationship between the types of γIMCs observed during severe invasive GAS infections and MDSCs, we investigated the ability of γIMCs to suppress T-cell responses. As reported previously, *in vitro*-differentiated Ly-6C$^+$ Ly-6G^{low} F4/80$^+$ MDSCs[9] spontaneously produced IFN-γ (Fig. 7a), and inhibited Ag-specific T-cell proliferation and IFN-γ production from T cells (Fig. 7b). Conversely, purified γIMCs failed to inhibit T-cell responses (Fig. 7c), suggesting that γIMCs are functionally distinct from MDSCs. Additionally, MDSCs markedly decreased in number and lost the ability to produce IFN-γ when cultured *in vitro* with severe invasive GAS isolates (Fig. 7a). Furthermore, CCR2$^-$ CX3CR1$^+$ CD31$^+$ γIMCs are phenotypically different from CCR2$^+$ CX3CR1$^-$ CD31$^-$ granulocytic MDSCs and CCR2^{high} CX3CR1$^-$ CD31$^+$ monocytic MDSCs (Supplementary

© 2012 Macmillan Publishers Limited. All rights reserved.

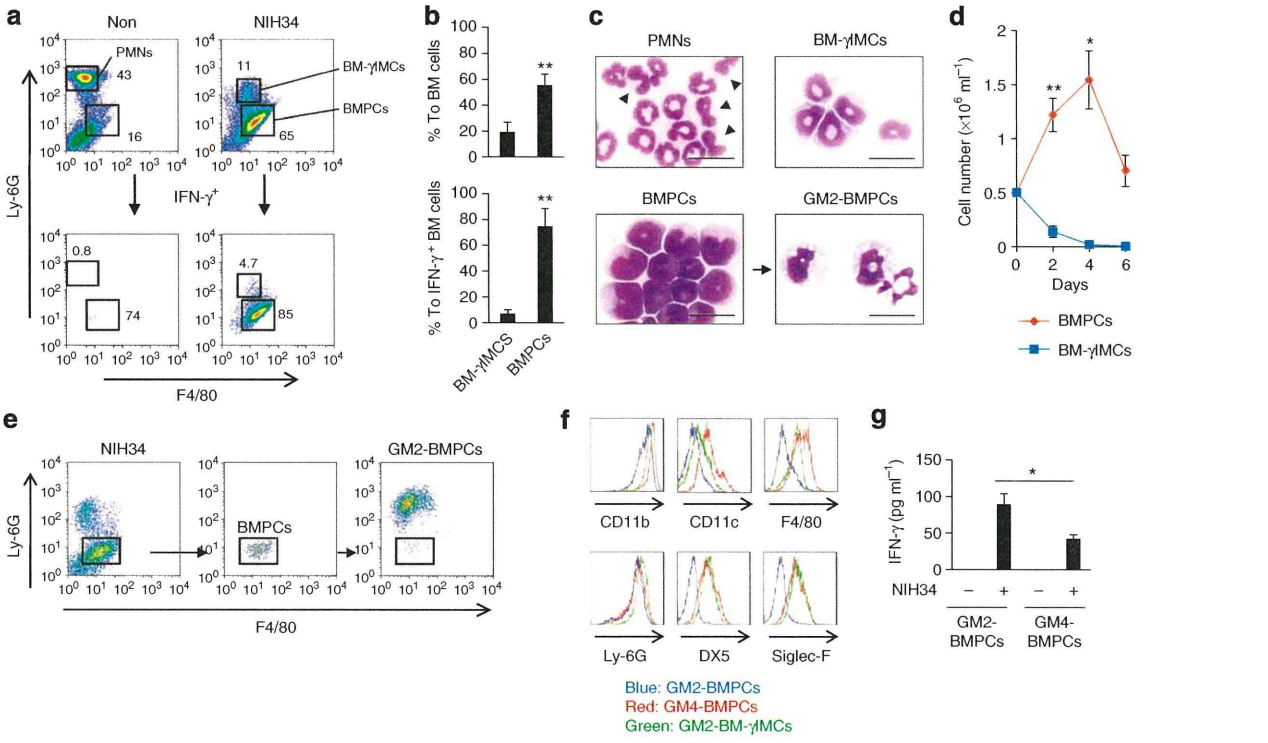

Figure 6 | BMPCs differentiate into γIMCs in the presence of GM-CSF. (**a**) C3H/HeN mice non-infected or i.p. infected with NIH34 (3.0×10^7 CFU per mouse) for 42 h were i.v. injected with monensin. Six hours later, the mice were killed and their bone marrow cells were immediately stained for the indicated markers, and analysed by ICS assay. Lower panels show the cells gated on the IFN-γ^+ population. The numbers (%) in the plots represent the proportion of PMNs, BM-γIMCs, and BMPCs to total (upper panels) and IFN-γ^+ (lower panels) bone marrow cells. (**b**) Proportion (%) of BM-γIMCs and BMPCs to bone marrow cells (upper panel) or IFN-γ-producing bone marrow cells (lower panel). Data are expressed as mean±s.d. ($n=3$). The differences compared with the proportion of BM-γIMCs were statistically significant (**$P<0.01$) as determined by Student's *t*-test. (**c**) Cytospin preparations of sorted PMNs, BM-γIMCs, BMPCs, and GM-CSF (2 days)-cultured BMPCs (GM2-BMPCs) were visualized with May-Grünwald-Giemsa staining. Arrowheads indicate stab neutrophils or metamyelocytes. Scale bars, 20 μm. (**d**) Sorted BMPCs and BM-γIMCs were cultured with GM-CSF (10 ng ml^{-1}) for 2–6 days, and their absolute numbers were counted on the indicated days. Data are expressed as mean±s.d. ($n=3$). The differences in proliferation increase were statistically significant (*$P<0.05$, **$P<0.01$) as determined by Student's *t*-test. (**e**) Flow cytometry profile of infected bone marrow cells (left), sorted BMPCs (middle), and GM2-BMPCs (right). Rectangles show a sorting gate of BMPCs. (**f**) GM-CSF-cultured BMPCs (2 days or 4 days; GM2-BMPCs, blue line; GM4-BMPCs, red line) and BM-γIMCs (2 days; GM2-BM-γIMCs, green line) were stained for the indicated markers. Data are representative of 3 independent experiments. (**g**) IFN-γ production from BMPCs. GM2-BMPCs or GM4-BMPCs were cultured with erythromycin-treated NIH34 (MOI 100) in the presence of control rat IgG or an IFN-γ neutralizing mAb (clone R4-6A2) for 24 h. The level of IFN-γ in the culture supernatants was measured by ELISA. The average (mean±s.d.) of triplicate wells is shown. Statistical significance (*$P<0.05$) was determined by Student's *t*-test.

Table S1). Taken together, our results indicate that γIMCs, which appear in association with severe invasive GAS infections, comprise a novel subset of IFN-γ-producing cells, but not MDSCs.

Role of γIMCs in severe invasive GAS infections. To elucidate the protective role of γIMCs, we employed an adoptive transfer system using WT or *Ifng*$^{-/-}$ mice. CD11b$^+$ CD11c$^-$ F4/80^{low} Ly-6G$^+$ γIMCs were purified from the spleens of WT mice infected with severe invasive GAS at day 2, and transferred into recipient mice. These mice were infected with a lethal dose of severe invasive GAS isolates (5×10^7 CFU (high dose)/WT mouse, 1×10^7 CFU (low dose)/*Ifng*$^{-/-}$ mouse), and the bacterial loads (CFUs) in the blood were quantified. At 24 h post-infection, γIMC-recipients and IFN-γ-treated mice had significantly lower bacterial loads in the blood than did control mice (Fig. 8a–c). Additionally, all control mice and all IFN-γ-treated mice died. By contrast, 100% of high dose-infected WT recipients and low dose-infected *Ifng*$^{-/-}$ recipients of γIMCs, and also low dose-infected WT mice, survived until 60 h post-infection (Fig. 8d–f). Our results indicate that IFN-γ successfully improved the bacterial clearance, but that systemic IFN-γ treatment was detrimental to survival following GAS infections (Fig. 8a,c,d and f). Thus, it appears that γIMCs have a protective role in severe invasive GAS infections.

Discussion

Previous studies have indicated that T cells and NK cells may have a role in the production of IFN-γ during GAS infections[5,15–17,19–21]. In the present study, we have demonstrated for the first time that γIMCs in the peritoneal cavity, skin, spleen, kidney, peripheral blood and bone marrow (but not T cells or NK cells) produce IFN-γ *in vivo* during the early stage of severe invasive GAS infections. The intensity of IFN-γ production is comparable among γIMCs, T cells, and NK cells, but production by γIMCs takes place sooner than that by T cells and NK cells. Moreover, throughout the course of GAS infection, γIMCs are the main IFN-γ-producing cells in the spleen. We further observed that IFN-γ neutralized *Rag*$^{-/-}$ mice succumbed to severe GAS infection at a similar rate to WT mice. Taken together, our results indicate that γIMCs comprise the major source of IFN-γ during the early stage of severe invasive GAS infections, and that they have an important protective role.

Notably, IFN-γ administration reduced the number of bacteria in the blood, whereas the transfer of γIMCs, but not of IFN-γ,

© 2012 Macmillan Publishers Limited. All rights reserved.

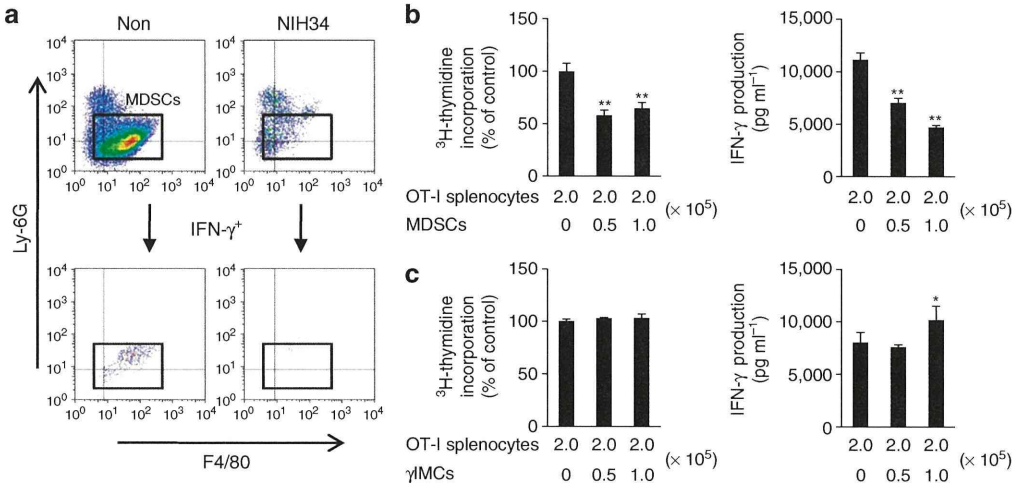

Figure 7 | γIMCs are functionally different from MDSCs. (**a**) C57BL/6 mouse bone marrow-derived MDSCs were differentiated *in vitro* with 40 ng ml^{-1} GM-CSF for 4 days. MDSCs were then incubated with or without severe invasive GAS isolates (NIH34; MOI 1) in the presence of brefeldin A (10 μg ml^{-1}). Three hours later, the cells were immediately stained for F4/80, Ly-6G, and IFN-γ, and analysed by ICS assay. Lower panels show the cells gated on the IFN-γ$^+$ population. (**b**,**c**) CD11b$^+$ CD11c$^-$ Ly-6C$^+$ Ly-6G^{low} *in vitro*-differentiated MDSCs, and CD11b$^+$ CD11c$^-$ F4/80^{low} Ly-6G$^+$ γIMCs, in the spleen from C57BL per six mice infected with NIH34 (3.0×10^7 CFU per mouse) for 48 h were isolated by FACS. Purified MDSCs (**b**) or purified γIMCs (**c**) were cultured at the indicated ratio with 2.0×10^5 splenocytes from C57BL/6.OT-I mice in the presence of antigenic $OVA_{357-364}$ peptides. Cell proliferation was measured using [^{3}H] thymidine uptake, and the level of IFN-γ in the culture supernatants was measured by ELISA. Each experiment was performed in triplicate. Mean±s.d. is shown. The differences compared with OT-I splenocytes alone were statistically significant (*$P<0.05$, **$P<0.01$) as determined by ANOVA. Data are representative of three independent experiments.

improved the survival rate of mice following GAS infection. Therefore, IFN-γ was necessary, but not sufficient, to protect mice from severe invasive GAS infections. We propose that NO production from γIMCs (which is restrictively controlled by IFN-γ), perhaps combined with that from other myeloid cells, may have a critical defensive role during the early stage of infection. In systemic GAS infection, γIMCs are deployed in various infected tissues; thus, the derived IFN-γ, NO, and/or as yet unidentified protective factors may promote the development of innate immune responses for the activation of phagocytes. However, we were unable to exclude the possibility that excessive quantities of IFN-γ secreted by T cells following superantigens stimulation, by NK cells, and even by γIMCs at the late stage of infection, are detrimental to survival following GAS infections, by exacerbating inflammatory responses and organ injury.

γIMCs express phenotypic markers of the monocyte/macrophage and granulocyte lineages, and are phenotypically different from other Ly-6C$^+$ cells, such as inflammatory and resident monocytes[11,36]. Mature PMNs, immature PMNs, and their progenitors proliferate or maintain their survival in the presence of G-CSF[37]. By contrast, in the present study, γIMCs did not survive in the presence of G-CSF. However, in the presence of GM-CSF, they differentiated into a PMN-like phenotype. Thus, γIMCs are distinct from the PMN lineage that develops during steady-state haematopoiesis. In the presence of GM-CSF, γIMCs possessed the ability to express a specific marker for Eos, Siglec-F. Nevertheless, based on staining with H7 and T21, they were distinct from Siglec-F$^+$ splenic Eos. Our observation that γIMCs failed to proliferate in response to IL-5 are consistent with the previous finding that T21 mAb may recognize IL-5Rα and other myeloid cell surface protein(s)[38]. Thus, γIMCs are unlikely to be committed to an Eos lineage; similarly, they are phenotypically different from DX5$^+$ basophils and basophil lineage-committed progenitors[39].

Granulocytic MDSCs are very similar to γIMCs in terms of surface markers (CD11b, F4/80, Ly-6C, Ly-6G, CD44, CD49d, and CD62L)[10,11], dependency on a growth factor (GM-CSF)[12], and cytokine production profile (IFN-γ)[13]. However, in the present study, we reveal that MDSCs did not produce IFN-γ in response to *in vitro* GAS infections. This is consistent with the previous finding that MDSCs from septic mice did not produce IFN-γ[40]. MDSCs are believed to originate from, or be accelerated by, the blockade of normal haematopoiesis during chronic inflammation or in a tumour-bearing state. γIMCs and MDSCs may therefore be closely related cell populations, and their differentiation and function may be regulated by the host circumstances.

On the basis of our present findings, we conclude that γIMCs are committed to an unclassified granulocyte lineage with an immature phenotype, and that such cells have the potential to replenish granulocyte populations. Moreover, GM-CSF is essential for the extraordinary state, such as severe systemic infection, but not for normal haematopoiesis[41]. The replacement of GM-CSF-dependent γIMCs may be regarded as a marked shift to the left of the leukocyte differential, with many immature granulocytes in automated cell counting. This is a characteristic of severe invasive GAS infections in our mouse model and also in human diseases[4,28]. The role of γIMCs in other infections and inflammatory diseases remains to be elucidated.

In the present study, we reveal that γIMCs differentiate from a subpopulation of CD11b$^+$ CD11c^{low} F4/80$^+$ Ly-6G^{low} cells in the bone marrow; this is known as a monocyte lineage. No γIMCs were detected in *Ifng*$^{-/-}$ mice infected with GAS, and IFN-γ-producing BMPCs (but not γIMCs) failed to differentiate into granulocyte-like cells in the presence of an IFN-γ neutralizing mAb. These observations suggest that the generation of γIMCs depends on the production of IFN-γ by BMPCs themselves. IFN-γ derived from BMPCs and γIMCs may be a key component of haematopoiesis during innate and adaptive immune responses, as shown in cases of malaria and *Mycobacterium avium* infection[35,42]. In the steady state, a few IFN-γ-producing cells existed in the Ly-6C^{low} CD31$^+$ fraction, including mixed progenitors of bone marrow[43]. Thus, we cannot exclude the possibility that BMPCs exist in non-infected bone marrow and have potential to produce IFN-γ, and that a subset of bone marrow cells can produce IFN-γ for the reproduction of haematopoietic stem cells[42].

© 2012 Macmillan Publishers Limited. All rights reserved.

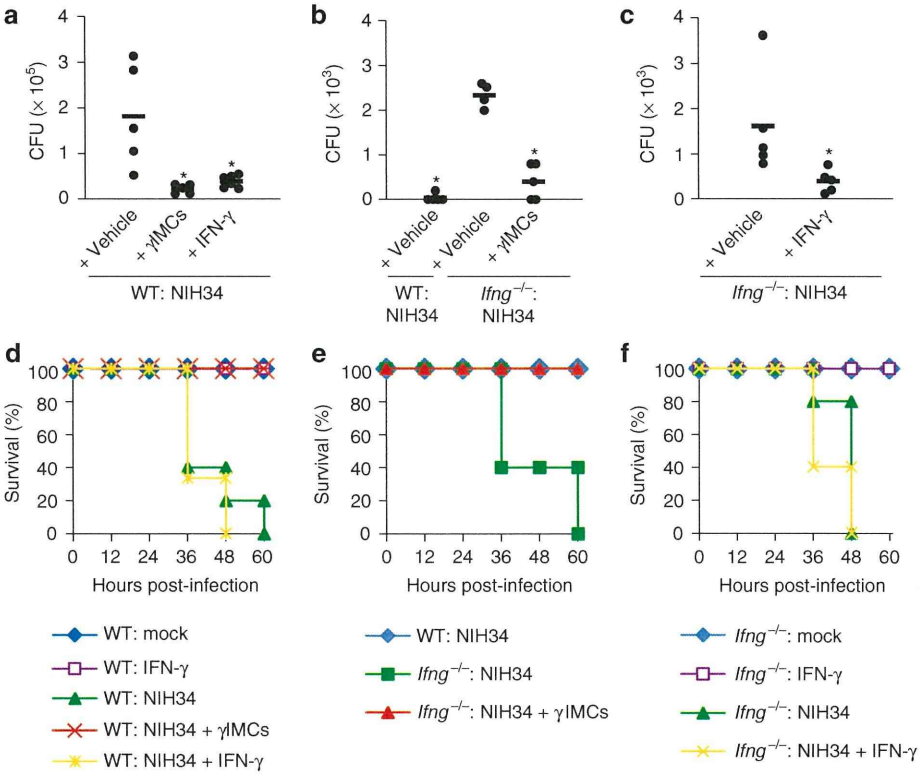

Figure 8 | γIMCs participate in protection against severe invasive GAS infections. (**a**–**f**) $CD11b^+$ $CD11c^-$ $F4/80^{low}$ $Ly\text{-}6G^+$ γIMCs in the spleen from C57BL/6 WT mice infected with NIH34 (3.0×10^7 CFU per mouse) for 48 h were isolated by FACS. WT or $Ifng^{-/-}$ mice i.v. received 3.0×10^6 γIMCs, or were i.p. treated with IFN-γ (10 ng per mouse). (**a**,**d**) WT mice ($n=5$), WT recipients of γIMCs ($n=5$), and mice i.p. treated with IFN-γ ($n=6$) were i.p. inoculated with NIH34 (5.0×10^7 CFU per mouse). (**b**,**e**) WT mice ($n=5$), $Ifng^{-/-}$ mice ($n=5$), and $Ifng^{-/-}$ recipients of γIMCs ($n=5$) were i.p. inoculated with NIH34 (1.0×10^7 CFU per mouse). (**c**,**f**) $Ifng^{-/-}$ mice ($n=5$) and $Ifng^{-/-}$ mice i.p. treated with IFN-γ ($n=5$) were i.p. inoculated with NIH34 (1.0×10^7 CFU per mouse). (**a**,**b**,**c**) The CFU of NIH34 in the peripheral blood was determined at 24 h post-infection. The differences compared with NIH34-infected WT mice (**a**) or NIH34-infected $Ifng^{-/-}$ mice (**b**,**c**) were statistically significant ($^*P<0.05$) as determined by the Mann–Whitney *U*-test. (**d**,**e**,**f**) Survival was observed for 60 h post-infection. Data are representative of two independent experiments.

Ring cells are present in the blood and bone marrow of humans, especially patients with chronic myeloproliferative diseases[6–8] but only rarely in healthy control subjects[7]. Further investigations of peripheral blood leukocytes or bone marrow cells from severe invasive GAS patients are required, to clarify whether the human counterpart of γIMCs is a major source of IFN-γ in STSS patients.

PMNs are known to be essential for protection against non-invasive streptococcal infections. Following infection with severe invasive strains, PMNs are impaired by enhanced virulence factors (for example, streptolysin O)[18,27], and therefore other protective mechanisms are required for the recovery. The results of our present study indicate that γIMCs, a novel class of differentiated granulocytic ring cells, which comprise the major source of IFN-γ during the early phase of severe invasive GAS infections, may have an important role. During the later stage of infection, IFN-γ derived from T cells and NK cells may be detrimental to the host. Nevertheless, we believe that the orchestrated regulation of γIMCs serves as a protective mechanism against severe invasive bacterial infections.

Methods

Bacterial strains. The STSS criteria in this study are based on those proposed by the Working Group on Severe Streptococcal Infections[44]. The clinical isolates from STSS (NIH34 (*emm3* genotype], NIH230 (*emm49* genotype), NIH186 (*emm1* genotype), and NIH202-2 (*emm1* genotype)), and also from non-invasive infections (K33 (*emm3* genotype)), were collected by the Working Group for Beta-hemolytic Streptococci in Japan[18,27].

Mice. All work performed using mice was carried out in accordance with the guidelines for animal care approved by National Institute of Infectious Diseases. C3H/HeN and C57BL/6 mice (male, 5–6-weeks-old) were purchased from SLC. C57BL/6.*Rag1*$^{-/-}$ (ref. 26) and C57BL/6.*Ifng*$^{-/-}$ (ref. 45) mice were purchased from the Jackson Laboratory. All mice were maintained in a specific pathogen-free condition.

GAS infections in a mouse model. GAS were grown to late-log phase (OD_{600} = 0.75–0.95). Then, 1.0×10^7 CFU to 5.0×10^7 CFU GAS, suspended in 0.5 ml PBS, were i.p. inoculated into 6–8-week-old male mice. In some experiments, mice were i.p. administered with 1 mg of an anti-mouse IFN-γ neutralizing mAb (clone R4-6A2) or control rat IgG, or 10 ng of recombinant mouse IFN-γ (Wako Pure Chemical Industries) at infection. Plasma production of CXCL10 (an IFN-γ-inducible protein) at 24 h, after NIH34 infection, was used to assess the activity of inoculated IFN-γ (10 ng per mouse) in $Ifng^{-/-}$ recipients ($Ifng^{-/-}$ mice, 230.1 ± 58.2 pg ml^{-1}; IFN-γ-treated $Ifng^{-/-}$ mice, 468.2 ± 147.2 pg ml^{-1}*; C57BL/6 mice as positive control, 460.6 ± 126.9 pg ml^{-1}*). Data were expressed as mean ± s.d. ($n=5$). The differences compared with $Ifng^{-/-}$ mice were statistically significant ($^*P<0.05$) as determined by Student's *t*-test. Survival curves were compared using a log-rank test.

Measurement of cytokines in plasma. The plasma cytokine levels were determined by FlowCytomix (eBioscience) using a FACSCalibur flow cytometer (Becton, Dickinson and Company (BD)), according to the manufacturer's instructions.

Flow cytometry analysis. For the *in vivo* ICS assay[22,23], at day 2 post-infection, mice were intravenously (i.v.) injected with 500 µl of a PBS solution containing 100 µg monensin (Sigma-Aldrich) at 6 h before collecting. Splenocytes, peripheral blood cells, bone marrow cells, and leukocytes in the peritoneal cavity, kidney, and skin were collected and rapidly processed on ice. Single-cell suspensions were prepared, and red blood cells were removed using an ammonium chloride lysis buffer. For the *in vitro* ICS assay, non-infected or infected cells were cultured with 10 µg ml^{-1} brefeldin A (Sigma-Aldrich) for 3 h. One million cells were stained with Alexa Fluor 488-, FITC-, PE-, Alexa Fluor 647-, allophycocyanin (APC)-, or Pacific Blue-conjugated Abs (clones and suppliers, Supplementary Table S2) at 4 °C for 15 min. Nonspecific staining was blocked with an anti-mouse FcγR mAb (clone 2.4G2). Dead cells were excluded by 7-aminoactinomycin D (7-AAD; Sigma-Aldrich) staining. After washing, cells were fixed in 2% paraformaldehyde/PBS for 10 min and then permeabilized in 0.5% saponin/0.5% BSA/PBS (permeabilization

© 2012 Macmillan Publishers Limited. All rights reserved.

buffer), before being stained with a PE- or APC-conjugated anti-mouse IFN-γ mAb (clone XMG1.2; eBioscience) or isotype control Ab (eBioscience) for 45 min at 4 °C. Cells were washed, first with permeabilization buffer, then with FACS buffer, before being applied to a FACSCalibur or FACSAria flow cytometer (BD). Analyses were performed using FlowJo software (Ashland, OR).

Cytological analysis. Fifty thousand cells were subjected to a cytospin (Thermo Shandon). For morphological analysis, the cytospin preparations were fixed with methanol and visualized with May-Grünwald-Giemsa staining. For intracellular IFN-γ staining, the cytospin preparations were fixed with 2% paraformaldehyde for 10 min, treated with 50 mM NH_4Cl/PBS for 15 min, and blocked with an anti-mouse FcγR mAb (clone 2.4G2) in permeabilization buffer for 15 min. Slides were stained with an APC-conjugated anti-mouse IFN-γ mAb (clone XMG1.2) or isotype control Ab (eBioscience) for 45 min, washed 3 times with permeabilization buffer, and then washed 3 times with PBS. Nuclei were visualized with propidium iodide staining. Samples were viewed and photographed with a Carl Zeiss LSM510 confocal laser scanning microscope.

Histology. For histological analysis, the tissues from GAS-infected mice were fixed in 10% formalin/PBS. The paraffin-embedded sections were stained with hematoxylin and eosin.

***In vitro* culture of γIMCs and BMPCs**. Purified CD11b$^+$ CD11c$^-$ F4/80^{low} Ly-6G$^+$ γIMCs and CD11b$^+$ CD11c^{low} F4/80$^+$ Ly-6G^{low} BMPCs from GAS-infected (monensin-untreated) mice were cultured at 0.5×10^6 cells per ml in medium containing RPMI 1640 (Wako) with 10% FBS (Nichirei), 100 U ml^{-1} penicillin, 10 μg ml^{-1} streptomycin, 2 mM glutamine, 25 mM HEPES, and 50 μM 2-ME, with or without 10–50 ng ml^{-1} recombinant mouse GM-CSF, G-CSF, M-CSF, or IL-5 (R&D Systems), in the presence or absence of 1 μg ml^{-1} control rat IgG or R4-6A2, for 2–6 days. On days 2 and 4, 50% of the medium was replaced with fresh medium, or the cells were collected for May-Grünwald-Giemsa staining and flow cytometry analysis. In some experiments, the cells were cultured at 0.5×10^6 cells ml^{-1} with 25 μg ml^{-1} erythromycin and NIH34 (MOI 100) in 10% FBS/phenol red-free RPMI medium, supplemented with 10 ng ml^{-1} GM-CSF, in the presence of 1 μg ml^{-1} control rat IgG or R4-6A2 for 24 h. The levels of IFN-γ and NO in the culture supernatants were measured by an instant ELISA kit (eBioscience) and a Griess reagent (Wako), respectively, according to the manufacturer's instructions.

***In vitro* culture of Eos and MDSCs**. For obtaining Eos, naïve bone marrow cells were cultured in 10% FBS/RPMI medium supplemented with stem cell factor (PeproTech) and FLT3-ligand (PeproTech) for 4 days, and then with medium containing recombinant mouse IL-5 (R&D Systems). On day 12, the cells were collected for May-Grünwald-Giemsa staining and flow cytometry analysis[46]. To isolate bone marrow-derived MDSCs, naïve bone marrow cells were cultured at 1.0×10^6 cells per ml in 10% FBS/RPMI medium, supplemented with 40 ng ml^{-1} GM-CSF. On day 4, the cells were collected for FACS analysis of CD11b$^+$ CD11c$^-$ Ly-6C$^+$ Ly-6G^{low} MDSCs[9].

Ag-specific T-cell proliferation and IFN-γ production. The Ag-specific proliferation of CD8$^+$ T cells was evaluated using OT-I OVA-specific MHC Class I-restricted TCR transgenic mice. Varying amounts of purified CD11b$^+$ CD11c$^-$ F4/80^{low} Ly-6G$^+$ γIMCs from infected C57BL/6 mice at 2 days post-infection, or bone marrow-derived F4/80$^+$ Ly-6C$^+$ Ly-6G^{low} MDSCs, were added to 2.0×10^5 naïve splenocytes from OT-I mice in medium containing RPMI 1640 with 10% FBS in a U-bottom 96-well plate. These co-cultures were stimulated with antigenic $OVA_{357-364}$ peptides (10 μM) for 4 days. Proliferation of OT-I cells in triplicate was estimated by the incorporation of [^{3}H] thymidine (1 μCi (0.0037 MBq) per well), added at 18 h before cell harvest. The level of IFN-γ in the culture supernatants was measured by an instant ELISA kit (eBioscience), according to the manufacturer's instructions.

Adoptive transfer of γIMCs. CD11b$^+$ CD11c$^-$ F4/80^{low} Ly-6G$^+$ γIMCs in splenocytes from *Ifng*$^{+/+}$ mice infected with NIH34 (3.0×10^7 CFU) for 48 h were isolated with a FACSAria flow cytometer. Recipient mice were i.v. administered with purified CD11b$^+$ CD11c$^-$ F4/80^{low} Ly-6G$^+$ γIMCs (3.0×10^6 cells), and i.p. inoculated with NIH34 (1.0×10^7 CFU to 5.0×10^7 CFU) on the same day.

Measurement of bacterial loads. At 24 h post-infection, 20 μl of peripheral blood was removed from the tail vein by phlebotomy. The blood was diluted at 1:10–1:1000 with PBS and spread on a Columbia agar plate containing 5% sheep blood (BD). To determine the number of NIH34 in peripheral blood, the plates were incubated for 20 h at 37 °C in a 5% CO_2 atmosphere, and the colonies were counted. The number of NIH34 was compared statistically using the Mann–Whitney *U*-test.

References

1. Lappin, E. & Ferguson, A. J. Gram-positive toxic shock syndromes. *Lancet Infect. Dis.* **9,** 281–290 (2009).
2. Cunningham, M. W. Pathogenesis of group A streptococcal infections. *Clin. Microbiol. Rev.* **13,** 470–511 (2000).
3. Davies, H. D *et al.* Invasive group A streptococcal infections in Ontario, Canada. Ontario Group A Streptococcal Study Group. *N. Engl. J. Med.* **335,** 547–554 (1996).
4. Bisno, A. L. & Stevens, D. L. Streptococcal infections of skin and soft tissues. *N. Engl. J. Med.* **334,** 240–245 (1996).
5. Raeder, R. H., Barker-Merrill, L., Lester, T., Boyle, M. D. & Metzger, D. W. A pivotal role for interferon-gamma in protection against group A streptococcal skin infection. *J. Infect. Dis.* **181,** 639–645 (2000).
6. Stavem, P., Hjort, P. F., Vogt, E. & van der Hagen, C. B. Ring-shaped nuclei of granulocytes in a patient with acute erythroleukaemia. *Scand. J. Haematol.* **6,** 31–32 (1969).
7. Langenhuijsen, M. M. Neutrophils with ring-shaped nuclei in myeloproliferative disease. *Br. J. Haematol.* **58,** 227–230 (1984).
8. Biermann, H. *et al.* Murine leukocytes with ring-shaped nuclei include granulocytes, monocytes, and their precursors. *J. Leukoc. Biol.* **65,** 217–231 (1999).
9. Rossner, S. *et al.* Myeloid dendritic cell precursors generated from bone marrow suppress T cell responses via cell contact and nitric oxide production *in vitro*. *Eur. J. Immunol.* **35,** 3533–3544 (2005).
10. Dardalhon, V. *et al.* Tim-3/galectin-9 pathway: regulation of Th1 immunity through promotion of CD11b+Ly-6G+ myeloid cells. *J. Immunol.* **185,** 1383–1392 (2010).
11. Movahedi, K. *et al.* Identification of discrete tumor-induced myeloid-derived suppressor cell subpopulations with distinct T cell-suppressive activity. *Blood* **111,** 4233–4244 (2008).
12. Youn, J. I., Nagaraj, S., Collazo, M. & Gabrilovich, D. I. Subsets of myeloid-derived suppressor cells in tumor-bearing mice. *J. Immunol.* **181,** 5791–5802 (2008).
13. Ribechini, E., Greifenberg, V., Sandwick, S. & Lutz, M. B. Subsets, expansion and activation of myeloid-derived suppressor cells. *Med. Microbiol. Immunol.* **199,** 273–281 (2010).
14. Medina, E., Goldmann, O., Rohde, M., Lengeling, A. & Chhatwal, G. S. Genetic control of susceptibility to group A streptococcal infection in mice. *J. Infect. Dis.* **184,** 846–852 (2001).
15. Goldmann, O., Chhatwal, G. S. & Medina, E. Immune mechanisms underlying host susceptibility to infection with group A streptococci. *J. Infect. Dis.* **187,** 854–861 (2003).
16. Goldmann, O. *et al.* The role of the MHC on resistance to group a streptococci in mice. *J. Immunol.* **175,** 3862–3872 (2005).
17. Goldmann, O., Chhatwal, G. S. & Medina, E. Contribution of natural killer cells to the pathogenesis of septic shock induced by Streptococcus pyogenes in mice. *J. Infect. Dis.* **191,** 1280–1286 (2005).
18. Ikebe, T. *et al.* Highly frequent mutations in negative regulators of multiple virulence genes in group A streptococcal toxic shock syndrome isolates. *PLoS Pathog.* **6,** e1000832 (2010).
19. Arad, G., Levy, R., Hillman, D. & Kaempfer, R. Superantigen antagonist protects against lethal shock and defines a new domain for T-cell activation. *Nat. Med.* **6,** 414–421 (2000).
20. Norrby-Teglund, A. *et al.* Evidence for superantigen involvement in severe group a streptococcal tissue infections. *J. Infect. Dis.* **184,** 853–860 (2001).
21. Kotb, M. *et al.* An immunogenetic and molecular basis for differences in outcomes of invasive group A streptococcal infections. *Nat. Med.* **8,** 1398–1404 (2002).
22. Liu, F. & Whitton, J. L. Cutting edge: re-evaluating the *in vivo* cytokine responses of CD8+ T cells during primary and secondary viral infections. *J. Immunol.* **174,** 5936–5940 (2005).
23. Sun, J., Madan, R., Karp, C. L. & Braciale, T. J. Effector T cells control lung inflammation during acute influenza virus infection by producing IL-10. *Nat. Med.* **15,** 277–284 (2009).
24. Nooh, M. M., El-Gengehi, N., Kansal, R., David, C. S. & Kotb, M. HLA transgenic mice provide evidence for a direct and dominant role of HLA class II variation in modulating the severity of streptococcal sepsis. *J. Immunol.* **178,** 3076–3083 (2007).
25. Abdeltawab, N. F. *et al.* An unbiased systems genetics approach to mapping genetic loci modulating susceptibility to severe streptococcal sepsis. *PLoS Pathog.* **4,** e1000042 (2008).
26. Mombaerts, P. *et al.* RAG-1-deficient mice have no mature B and T lymphocytes. *Cell* **68,** 869–877 (1992).
27. Ato, M., Ikebe, T., Kawabata, H., Takemori, T. & Watanabe, H. Incompetence of neutrophils to invasive group A streptococcus is attributed to induction of plural virulence factors by dysfunction of a regulator. *PLoS One* **3,** e3455 (2008).
28. Eriksson, B. K., Andersson, J., Holm, S. E. & Norgren, M. Epidemiological and clinical aspects of invasive group A streptococcal infections and the streptococcal toxic shock syndrome. *Clin. Infect. Dis.* **27,** 1428–1436 (1998).
29. Iwasaki, H. *et al.* Identification of eosinophil lineage-committed progenitors in the murine bone marrow. *J. Exp. Med.* **201,** 1891–1897 (2005).

© 2012 Macmillan Publishers Limited. All rights reserved.

30. Angulo, I. *et al.* Involvement of nitric oxide in bone marrow-derived natural suppressor activity. Its dependence on IFN-gamma. *J. Immunol.* **155,** 15–26 (1995).
31. Angulo, I. *et al.* Early myeloid cells are high producers of nitric oxide upon CD40 plus IFN-gamma stimulation through a mechanism dependent on endogenous TNF-alpha and IL-1alpha. *Eur. J. Immunol.* **30,** 1263–1271 (2000).
32. Pelaez, B., Campillo, J. A., Lopez-Asenjo, J. A. & Subiza, J. L. Cyclophosphamide induces the development of early myeloid cells suppressing tumor cell growth by a nitric oxide-dependent mechanism. *J. Immunol.* **166,** 6608–6615 (2001).
33. Campillo, J. A., Pelaez, B., Angulo, I., Bensussan, A. & Subiza, J. L. Involvement of IFNbeta on IFNgamma and nitric oxide (NO) production by bone marrow (BM) cells in response to lipopolysaccharide. *Biomed. Pharmacother.* **60,** 541–547 (2006).
34. Gallina, G. *et al.* Tumors induce a subset of inflammatory monocytes with immunosuppressive activity on CD8+ T cells. *J. Clin. Invest.* **116,** 2777–2790 (2006).
35. Belyaev, N. N. *et al.* Induction of an IL7-R(+)c-Kit(hi) myelolymphoid progenitor critically dependent on IFN-gamma signaling during acute malaria. *Nat. Immunol.* **11,** 477–485 (2010).
36. Serbina, N. V., Jia, T., Hohl, T. M. & Pamer, E. G. Monocyte-mediated defense against microbial pathogens. *Annu. Rev. Immunol.* **26,** 421–452 (2008).
37. Metcalf, D. & Nicola, N. A. Proliferative effects of purified granulocyte colony-stimulating factor (G-CSF) on normal mouse hemopoietic cells. *J. Cell. Physiol.* **116,** 198–206 (1983).
38. Hitoshi, Y. *et al.* Distribution of IL-5 receptor-positive B cells. Expression of IL-5 receptor on Ly-1(CD5)+ B cells. *J. Immunol.* **144,** 4218–4225 (1990).
39. Lee, J. J. & McGarry, M. P. When is a mouse basophil not a basophil? *Blood* **109,** 859–861 (2007).
40. Delano, M. J. *et al.* MyD88-dependent expansion of an immature GR-1(+) CD11b(+) population induces T cell suppression and Th2 polarization in sepsis. *J. Exp. Med.* **204,** 1463–1474 (2007).
41. Zhan, Y., Lieschke, G. J., Grail, D., Dunn, A. R. & Cheers, C. Essential roles for granulocyte-macrophage colony-stimulating factor (GM-CSF) and G-CSF in the sustained hematopoietic response of Listeria monocytogenes-infected mice. *Blood* **91,** 863–869 (1998).
42. Baldridge, M. T., King, K. Y., Boles, N. C., Weksberg, D. C. & Goodell, M. A. Quiescent haematopoietic stem cells are activated by IFN-gamma in response to chronic infection. *Nature* **465,** 793–797 (2010).
43. Trottier, M. D., Newsted, M. M., King, L. E. & Fraker, P. J. Natural glucocorticoids induce expansion of all developmental stages of murine bone marrow granulocytes without inhibiting function. *Proc. Natl Acad. Sci. USA* **105,** 2028–2033 (2008).
44. Breiman, R. F. *et al.* Defining the group A streptococcal toxic shock syndrome. Rationale and consensus definition. *JAMA* **269,** 390–391 (1993).
45. Dalton, D. K. *et al.* Multiple defects of immune cell function in mice with disrupted interferon-gamma genes. *Science* **259,** 1739–1742 (1993).
46. Dyer, K. D. *et al.* Functionally competent eosinophils differentiated *ex vivo* in high purity from normal mouse bone marrow. *J. Immunol.* **181,** 4004–4009 (2008).

Acknowledgements

We thank Dr. Satoshi Takaki (Research Institute National Center for Global Health and Medicine) and Dr. Kiyoshi Takatsu (University of Toyama) for providing the anti-IL-5Rα mAb (clone H7); Dr. Akihiko Yoshimura (Keio University) for providing the anti-IFN-γ mAb; Dr. Hideki Fujii and Dr. Shigeo Koyasu (Keio University) for providing the OT-I transgenic mice; Dr. Paul M. Kaye (University of York) for critical comments; and Ms Yoko Nakamura for technical assistance. This work was partly supported by a grant (H22-Shinkou-Ippan-013 to M.A., T.I., and H.W.) from the Ministry of Health, Labour and Welfare of Japan, and by a Grant-in-Aid for Young Scientists (B) (22790959 to T.M.) from the Japan Society for the Promotion of Science.

Author contributions

T.M., M.A., and T.I. designed and performed the experiments. T.M. and M.A. analysed the data. T.M., M.A., T.I., M.O., H.W. and K.K. wrote the manuscript.

Additional information

Supplementary Information accompanies this paper at http://www.nature.com/naturecommunications

Competing financial interests: The authors declare no competing financial interests.

Reprints and permission information is available online at http://npg.nature.com/reprintsandpermissions/

How to cite this article: Matsumura, T. *et al.* Interferon-γ-producing immature myeloid cells confer protection against severe invasive group A *Streptococcus* infections *Nat. Commun.* 3:678 doi: 10.1038/ncomms1677 (2012).

License: This work is licensed under a Creative Commons Attribution-NonCommercial-NoDerivative Works 3.0 Unported License. To view a copy of this license, visit http://creativecommons.org/licenses/by-nc-nd/3.0/

© 2012 Macmillan Publishers Limited. All rights reserved.

Shimomura et al. BMC Genomics 2011, 12:17
http://www.biomedcentral.com/1471-2164/12/17

BMC Genomics

RESEARCH ARTICLE Open Access

Complete genome sequencing and analysis of a Lancefield group G *Streptococcus dysgalactiae* subsp. *equisimilis* strain causing streptococcal toxic shock syndrome (STSS)

Yumi Shimomura[1], Kayo Okumura[1,4], Somay Yamagata Murayama[2], Junji Yagi[3], Kimiko Ubukata[2], Teruo Kirikae[1], Tohru Miyoshi-Akiyama[1*]

Abstract

Background: *Streptococcus dysgalactiae* subsp. *equisimilis* (SDSE) causes invasive streptococcal infections, including streptococcal toxic shock syndrome (STSS), as does Lancefield group A *Streptococcus pyogenes* (GAS). We sequenced the entire genome of SDSE strain GGS_124 isolated from a patient with STSS.

Results: We found that GGS_124 consisted of a circular genome of 2,106,340 bp. Comparative analyses among bacterial genomes indicated that GGS_124 was most closely related to GAS. GGS_124 and GAS, but not other streptococci, shared a number of virulence factor genes, including genes encoding streptolysin O, NADase, and streptokinase A, distantly related to SIC (DRS), suggesting the importance of these factors in the development of invasive disease. GGS_124 contained 3 prophages, with one containing a virulence factor gene for streptodornase. All 3 prophages were significantly similar to GAS prophages that carry virulence factor genes, indicating that these prophages had transferred these genes between pathogens. SDSE was found to contain a gene encoding a superantigen, streptococcal exotoxin type G, but lacked several genes present in GAS that encode virulence factors, such as other superantigens, cysteine protease *speB*, and hyaluronan synthase operon *hasABC*. Similar to GGS_124, the SDSE strains contained larger numbers of clustered, regularly interspaced, short palindromic repeats (CRISPR) spacers than did GAS, suggesting that horizontal gene transfer via streptococcal phages between SDSE and GAS is somewhat restricted, although they share phage species.

Conclusion: Genome wide comparisons of SDSE with GAS indicate that SDSE is closely and quantitatively related to GAS. SDSE, however, lacks several virulence factors of GAS, including superantigens, SPE-B and the *hasABC* operon. CRISPR spacers may limit the horizontal transfer of phage encoded GAS virulence genes into SDSE. These findings may provide clues for dissecting the pathological roles of the virulence factors in SDSE and GAS that cause STSS.

Background

Since Lancefield group G streptococci (GGS) have been considered components of the normal flora of the human throat, skin, and genitourinary tract, the contributions of GGS to streptococcal disease have often been overlooked [1]. Over the last decade, however, infections by pathogenic GGS have been reported, including life-threatening invasive β-hemolytic streptococcal disease [1-7], making it necessary to expand our knowledge of the pathogenesis of GGS infections, especially invasive infections. Several species of streptococci can carry group C and G antigens, including *Streptococcus dysgalactiae* subsp. *equisimilis* (SDSE), *S. canis*, *S. dysgalactiae* subsp. *dysgalactiae*, *S. equi* subsp. *equi* (SESE), *S. equi* subsp. *zooepidemicus* (SESZ), and *S. anginosus* group bacteria. SDSE, which consists of Lancefield group G and C bacteria, in a ratio of about 4:1 [3,8,9], has been isolated from patients at higher frequency than

* Correspondence: takiyam@ri.ncgm.go.jp
[1]Department of Infectious Diseases, National Center for Global Health and Medicine, 1-21-1, Toyama, Shinjuku-ku, Tokyo 162-8655, Japan
Full list of author information is available at the end of the article

BioMed Central

© 2011 Shimomura et al; licensee BioMed Central Ltd. This is an Open Access article distributed under the terms of the Creative Commons Attribution License (http://creativecommons.org/licenses/by/2.0), which permits unrestricted use, distribution, and reproduction in any medium, provided the original work is properly cited.

other GGS and GCS species. For example, of 313 strains of GCS and GGS isolated from clinical samples in Southern India between 2006 and 2007, 254 (81.1%) were SDSE [9], as were 80% of the 266 invasive non-A and non-B β-hemolytic streptococcal isolates in the USA [3]. The spectrum and clinical courses of SDSE infection, including pharyngitis, cellulitis, infective arthritis, vertebral osteomyelitis, and streptococcal toxic shock syndrome (STSS), show substantial overlap with those of GAS [10-16]. Despite the increased clinical importance of SDSE, however, the entire SDSE genome has not yet been sequenced. Knowledge of its entire genome sequence is fundamental to gain insights into the pathogenicity of SDSE. We describe here the entire genome sequence of a Lancefield group G SDSE strain, GGS_124, which had been isolated from a patient with STSS.

Results

Selection of an SDSE isolate for genome sequencing

We chose a clinical isolate of SDSE, strain GGS_124, for genome sequence determination for several reasons. First, GGS_124 belongs to Lancefield group G, to which most clinical isolates of SDSE also belong [3,8,9]. Second, GGS_124 caused STSS in a patient. Third, GGS_124 was the most virulent strain among 8 group G SDSE isolates, as determined by their LD_{50} values in a mouse infection model (Table 1).

Overview of the SDSE GGS_124 genome sequence

We found that, similar to other streptococcal genomes, the SDSE GGS_124 genome consists of a single circular chromosome of 2,106,340 bp (Additional file 1) and has a G+C content of 39.6% (Figure 1). Based on its location in the intergenic region upstream of the *dnaA* gene (SDEG_0001), the GC skew, and the clustering of dnaA box motifs, the start point of the SDSE GGS_124 genome was assigned to the putative origin of replication (*oriC*). An AT-rich 13-mer (AGTCTGTTTTTTT), located in the intergenic region upstream of the *dnaA* gene [17], was selected as the starting point for nucleotide numbering. The GGS_124 genome was shown to contain 2095 predicted coding sequences (CDS), which account for 1.83 Mbp (86.9%) of the genome. In addition, this genome was shown to harbor 3 prophage-like elements, designated ΦGGS_124.1, ΦGGS_124.2, and ΦGGS_124.3. Moreover, there were 27 insertion sequence (IS) elements throughout the genome.

Table 1 *emm* types and mouse LD_{50} values of 8 SDSE isolates used in this study

Strain	Origin	Symptom STSS/Non-STSS	LD_{50} value (CFU/head)	*emm* type
GGS_124	human	STSS	2.1×10^6	*stG480.0*
168	human		4.6×10^6	*stG480.0*
GGS_117	human	STSS	5.6×10^6	*stG4974.1*
170	human		5.6×10^6	*stC36.0*
164	human		1.9×10^7	*stG485*
GGS_118	human	STSS	2.0×10^7	*stG67920*
169	human		4.4×10^7	*stG11*
163	human		4.5×10^7	*stG643*

LD_{50} values of the isolates were determined as described in MATERIALS AND METHODS.

Genome sequence homology analysis of GGS_124 with the other 11 sequenced streptococcal species and subspecies showed that GGS_124 was closest in sequence to GAS, with 72% similarity (Additional file 1). GGS_124 was less similar to SESZ and SESE, with 65% and 64% coverage. Although *S. agalactiae* is the closest-relatiIve of SDSE based on 16S rRNA analysis, the *S. agalactiae* strains were less similar to SDSE than GAS based on the genome wide comparison (Additional file 1). In addition, we constructed a phylogenetic tree of all sequenced *Streptococcus* species based on the neighbor-joining method (Additional file 2). Although neighbor-joining methods are less accurate than the other methods such as most likelihood methods, SDSE is clustered with the GAS strains as their closest relative.

We compared the gene organization of GGS_124 with that of GAS by genomic rearrangement analyses (Figure 2 and Additional file 3). GAS could be divided roughly into 2 groups according to the orientation of the genes [18,19]. Therefore, SSI-1 and MGAS315, both of which are M3 serotype strains and have opposite gene orientations from each other, were chosen for the analysis. We found that the GGS_124 genome was organizationally more similar to that of GAS strain MGAS315 than GAS strain SSI-1 (Figure 2). Interestingly, the colinearity of GGS_124 and *S. uberis* genomes was quite remarkable but the percent amino acid identity was lower than that of the GAS strains (Additional file 3). The gene structure of GGS_124 was similar to the structures of GAS strain SSI-1, SESZ strain MGCS10565, and SESE strain 4047, although the GGS_124 genome contains large-scale genomic rearrangements. The GGS_124 genome differed markedly in gene organization from the genome of GBS strain A909.

When we compared genes from GGS_124 and two relatively homologous species, GAS (MGAS315) and SESZ (MGCS10565) (Figure 3), we found that these three streptococcal genomes contain more than 1,200 orthologous genes, accounting for 59% of the total CDSs of GGS_124. GGS_124 shares 282 genes with MGAS315 and 153 genes with MGCS10565. Moreover, 71.6% of the genes of GGS_124 were homologous to GAS genes, with 88.5% amino acid identity, whereas 66.5% of GGS_124 genes were homologous to MGCS10565

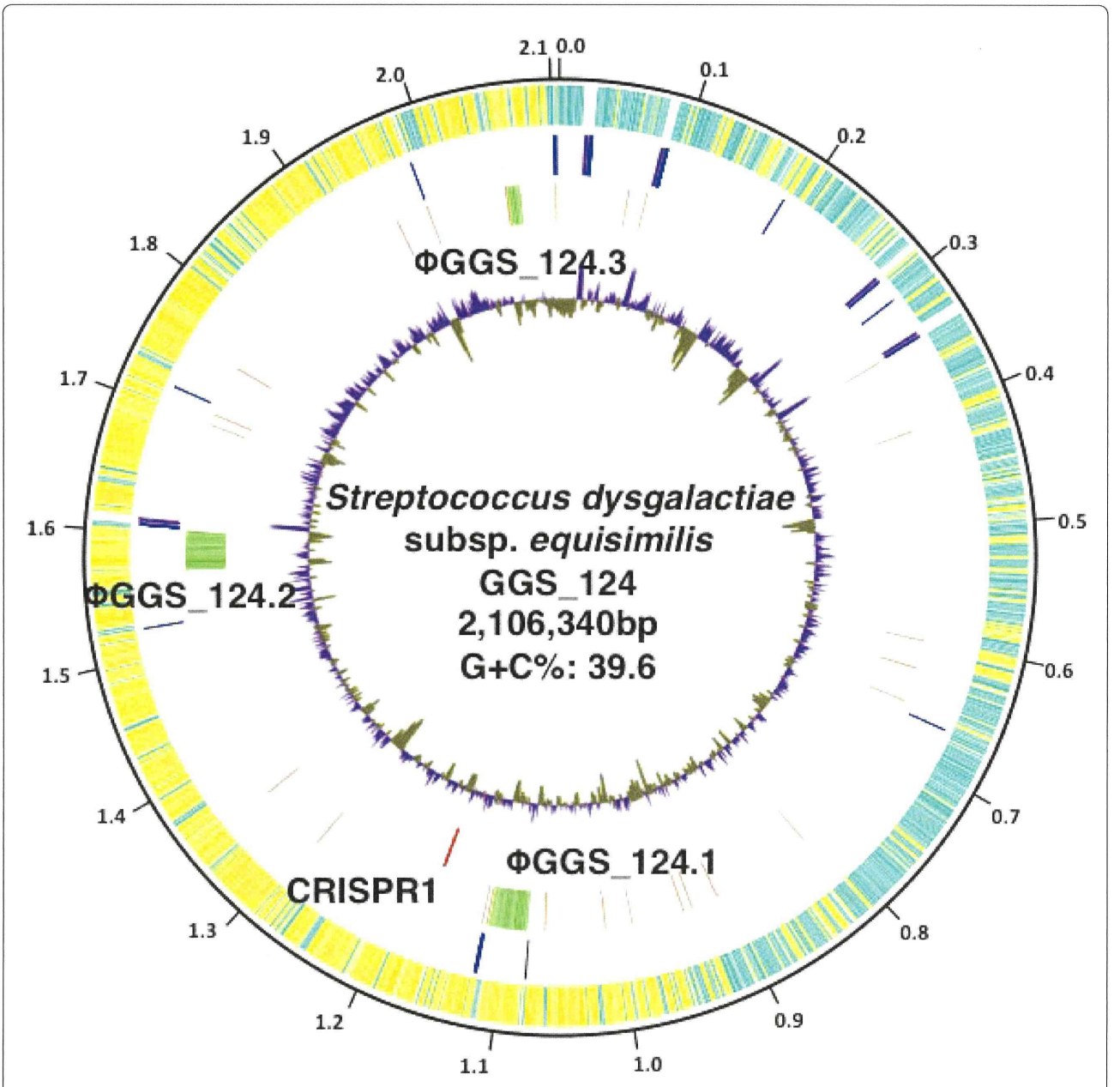

Figure 1 Circular representation of the genome of *S. dysgalactiae* subsp. *Equisimilis* strain GGS_124. Circle 1 (outermost circle) indicates the distance from the putative origin of replication. Circle 2 shows annotated CDS encoded on the forward (light blue) and reverse (yellow) chromosomal strands, respectively. The rRNA genes (pink), tRNA genes (blue), and tmRNA gene (black) are shown in circle 3. Prophage (green) and ISs (orange) genes are shown in circle 4. CRISPR (red) is shown in circle 5. Circle 6 (innermost circle) shows the G+C content with greater and less than average (0.40) in purple and brown, respectively.

genes, with 79.9% amino acid identity. These findings indicate that SDSE is closely related to GAS in both nucleotide and amino acid sequences.

We also analyzed the distribution of genes shown to be more homologous to genes derived from bacteria other than GAS (Additional file 4). We found that 299 genes showed higher similarity to genes from *Streptococci* other than GAS and 92 genes showed higher similarity to genes from a genus other than *Streptococcus*. In addition, we identified 11 genes that did not show significant homology to any genes in the databases. These genes were scattered throughout the entire GGS_124 genome, suggesting that they had not been acquired by massive genome recombination.

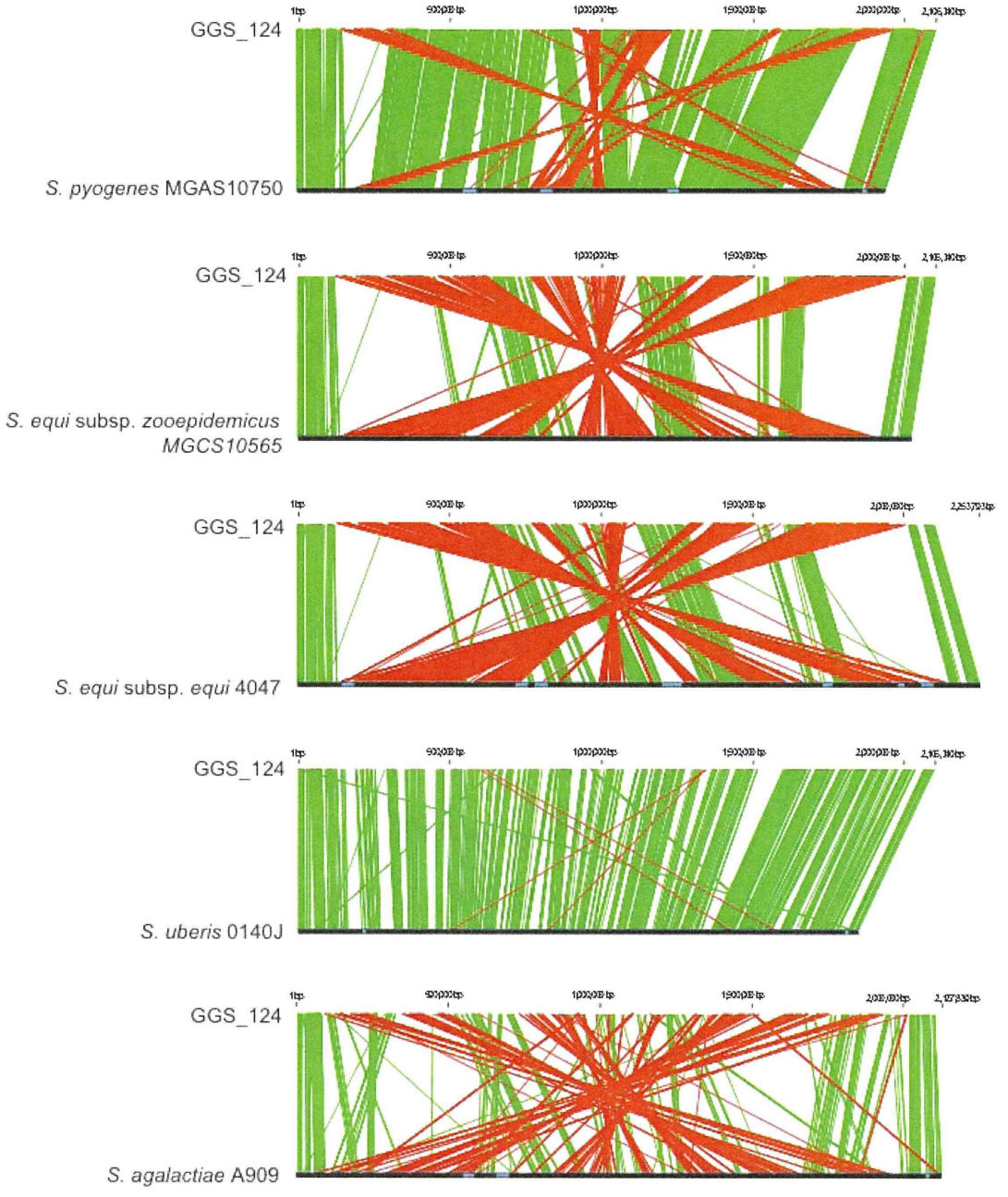

Figure 2 Genome rearrangement maps of *S. dysgalactiae* subsp. *equisimilis* GGS_124 with five species in the pyogenic group. Sequences were aligned from the predicted replication origin of each genome. The colored bars separating each genome (red and green) represent similarity matches identified by *in silico* Molecular Cloning. Links shown in green match in the same orientation, while those in red match in the reverse orientation. Prophages are highlighted as pale blue boxes.

Putative prophages and CRISPR/Cas

We found that all three prophage-like elements of GGS_124 were homologous to previously sequenced GAS prophages, and that they were integrated at sites similar to those of GAS strains, with the same upstream and downstream genes (Figure 4).

(i) Prophage GGS_124.1

We found that the ΦGGS_124.1 prophage is 35.593 bp in length with a G+C content of 38.04% and carries 60 CDS. Ninety-seven percent of the CDS in ΦGGS_124.1 have homologues, with more than 40% identity to GAS prophages, suggesting that ΦGGS_124.1 is a chimeric

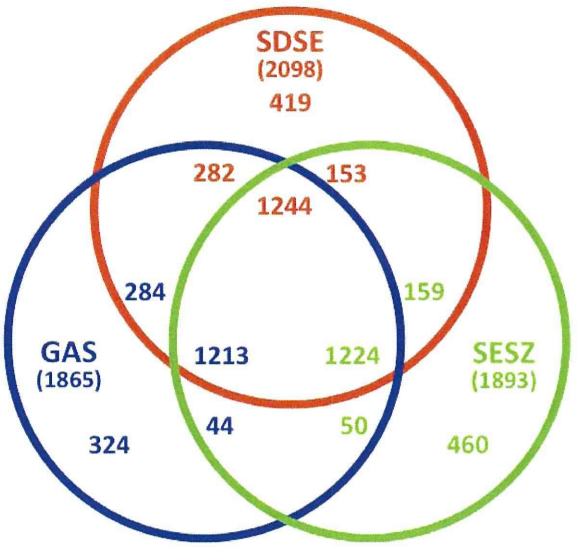

Figure 3 Venn diagram of gene content comparison among *S. dysgalactiae* subsp. *equisimilis* GGS_124 (SDSE), *S. pyogenes* MGAS315 (GAS) and SESZ MGCS10565. The inferred proteomes of SDSE, GAS, and SESZ were compared in a pairwise manner with their translated genomes by *in silico* Molecular Cloning and are presented as a Venn diagram. The numbers of products for each section are color coded to match the respective genomes. Genes showing more than 40% identity were considered homologues.

phage. This prophage was inserted at the predicted bacteriophage T12*att* site, which has been shown to be a gene that encodes a serine tRNA and is located between the CDS of SDEG_1100 and SDEG_1161 [20]. Six GAS strains, MGAS10394, MGAS315, MGAS5005, MGAS6180, MGAS8232, and SSI-1, have prophage elements: Φ10394.3, which carries *speK* and the streptococcal phospholipase A2 gene (*sla*); Φ315.2, which carries *ssa*; Φ5005.1, which carries *speA*; Φ6180.1, which carries the *speC* and Dnase (*spd*) genes; Φ8232.3, which carries *speL* and *speM*; and SPsP5, which carries *speC*, respectively [18,21-25]. In addition, ΦGGS_124.1 was found to contain a prophage-associated virulence factor gene for deoxyribonuclease (*sdc*).

(ii) Prophage GGS_124.2

We found that the ΦGGS_124.2 prophage is 35,814 bp in length, with a G+C content of 38.20% and 61 CDS. Ninety-five percent of the CDS in ΦGGS_124.1 have homology with genes in GAS prophages, making it likely that ΦGGS_124.2 is chimeric phage. The chromosomal phage attachment site (*attB*) and the ΦGGS_124.2 phage-encoded attachment site (*attP*) were not found, but the products of *attP/attB* recombination, *attL* and *attR*, with the same sequences as those of GAS prophages SPsP2 and Φ315.5 were identified. The genome context around the integration site for ΦGGS_124.2 was found to be conserved at the phage integration sites of 4 GAS strains, MGAS10394, MGAS315, SSI-1, and Manfredo, which contain the prophage elements Φ10394.6, carrying *sdn*; Φ315.5, carrying *speA*; SPsP2, carrying *speA*; and phiMan.1, carrying the DNase gene *mf3*, respectively [18,19,21,22]. No known prophage-associated virulence factor genes were found in ΦGGS_124.2.

(iii) Prophage GGS_124.3

We also found a prophage remnant, ΦGGS_124.3, which was about 12.6 kb length and homologous to the previously sequenced GAS prophage remnants Φ6180.4 and Φ10270.5 with a nucleotide identity of 73%. ΦGGS_124.3 and the two GAS phage remnants were found to be located between genes encoding a putative transcriptional regulator protein and the 30S ribosomal protein. In strain GGS_124, two truncated transposase proteins, SDEG_2117 and SDEG_2118, were found to be inserted upstream of GGS_124.3. No virulence factor genes are present in GGS_124.3.

Prokaryotes possess a system that mediates resistance to infection by foreign DNA, such as viruses [26,27]. When bacteria are exposed to phages, short fragments derived from phage DNA are integrated into clusters of regularly interspaced short palindromic repeat (CRISPR) regions of the bacterial genome as spacers [27]. CRISPR RNA transcripts and CRISR-associated proteins (Cas), act in complexes to interfere with virus proliferation [26]. This system has also been observed in GAS [20], SESZ [22,28], *S. mutans* [29], and *S. thermophilus* [30]. GGS_124 harbors a CRISPR/Cas system consisting of an array of genes, *can1*, *cas1*, *cas2*, and *csn2*, and CRISPR (Figure 5). The GGS_124 CRISPR has 19 direct repeats of 36 bp each and 18 spacer sequences 30 or 32 bp in length; 6 of these sequences are homologous to GAS prophage sequences, with more than 80% coverage (Additional file 5). When we analyzed the number of CRISPR spacers in an additional 7 SDSE isolates (Table 2), we found that the mean number of CRISPR spacers was higher in SDSE (18.0 ± 3.3 spacers) than in GAS strains (4.0 ± 1.0 spacers; range, 0 to 9) (Table 2). These results suggest that prophage infection of SDSE is somewhat restricted, resulting in a smaller number of virulence factors located in the prophage regions of SDSE. Alternatively, SDSE may be in contact with phages more frequently, with integrated phages having a fitness cost for SDSE.

Virulence factors encoded by the GGS_124 genome

An analysis of 58 SDSE strains isolated from human infections using targeted microarrays containing 216 GAS virulence genes composed of 70mer oligonucleotides showed that about 50% of the GAS virulence genes represented in the microarray were present in SDSE [31]. Three molecular markers, *speB*, the intergenic region upstream of the *scpG* gene and *virPCR*, have

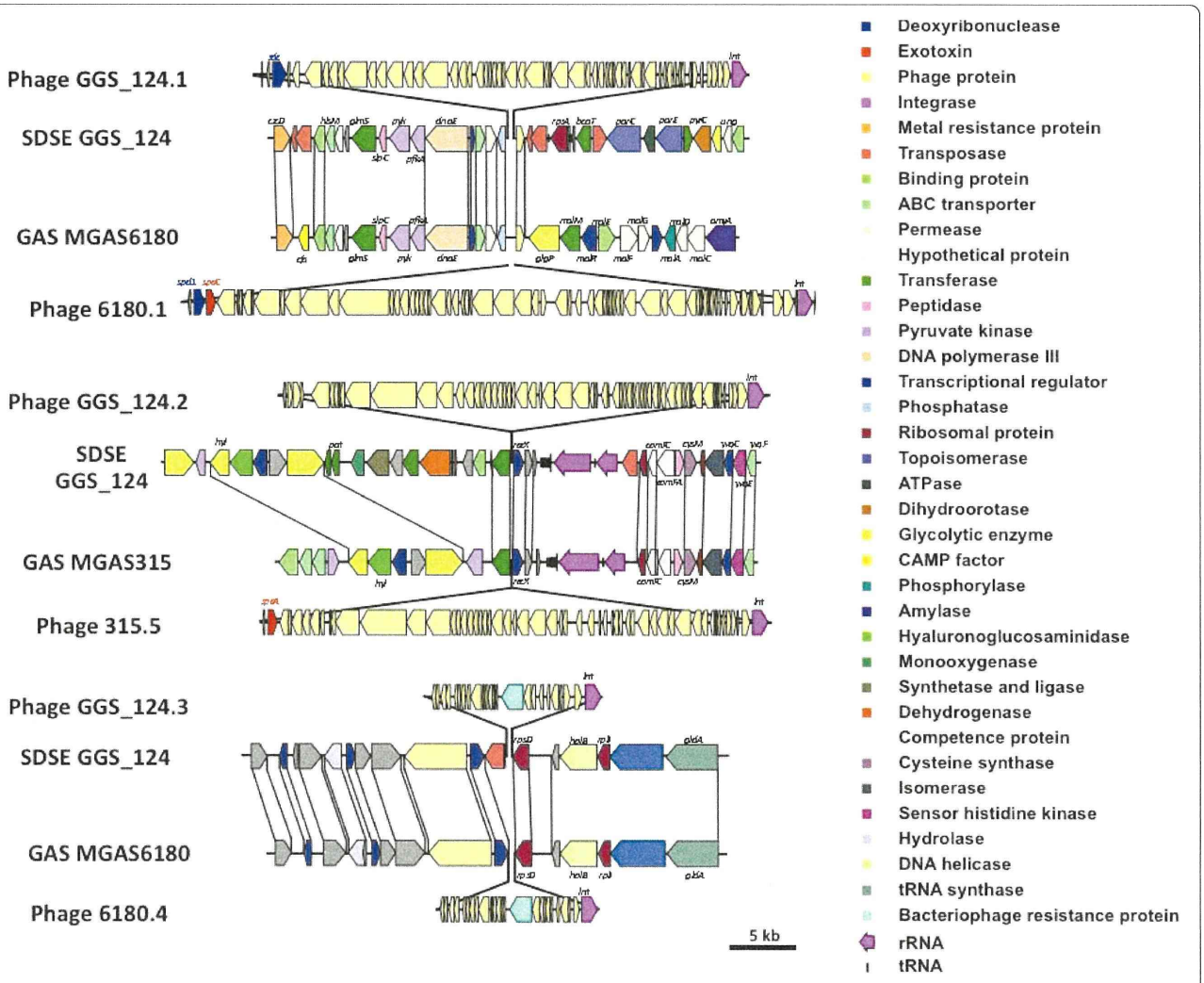

Figure 4 Prophage elements and the surrounding gene arrangements of GGS_124 and GAS. The organization of the genes located in the putative prophage regions found in GGS_124 and their insertion points in the genome were compared with those of GAS. Colored boxes between genes indicate level of similarity at the amino acid level (red, ≥90%; orange, 89%-80%; green, 79%-70%).

been shown helpful in discriminating between GAS and SDSE [32]. Based on homology analyses with known bacterial virulence factors, such as pore-forming toxins, a superantigen, proteases, FCT-like regions, adhesins, hyaluronidase, and a nuclease, we identified 71 putative virulence factor genes in the GGS_124 genome; their details are shown in Additional file 6. Comparison of the virulence factors in GGS_124 with those of other streptococcal species indicated that the putative virulence factors most similar to those of GGS_124 were found in GAS. In contrast, superantigen, SPE-B and the *has* operon of GAS are not conserved in GGS_124.

(i). Pore-forming toxins

GGS_124 has several putative hemolysins, including HlyX (SDEG_0427), HlyIII (SDEG_1015), and HlyA1 (SDEG_1483), which have also been detected in GAS, SESZ, SESE, *S. uberis*, and GBS. GGS_124 also has genes encoding streptolysin S (*sagA*) (SDEG_0705) and its biosynthesis proteins (*sagBCDEFGHI*) (SDEG_0706 to 0713), which are also present in GAS [33], SESZ, and SESE [22,28,34]. In addition, GGS_124 carries a gene for streptolysin O (SLO) (SDEG_2027), which is essential for GAS virulence and is required for the organism to escape from the endosome into the cytosol following invasion of host cells [35].

(ii). Superantigen

GGS_124 possesses only one superantigen gene, exotoxin G variant 4 (*spegg4*), which is homologous to GAS streptococcal exotoxin G (SpeG), with 79% amino acid identity (Additional file 6). In a previous analysis of the superantigenic activities of the *spegg4* product in human peripheral blood mononuclear cells [36], we found that its mitogenic activity was about 1% that of SpeG from GAS. Other genome-encoded superantigen

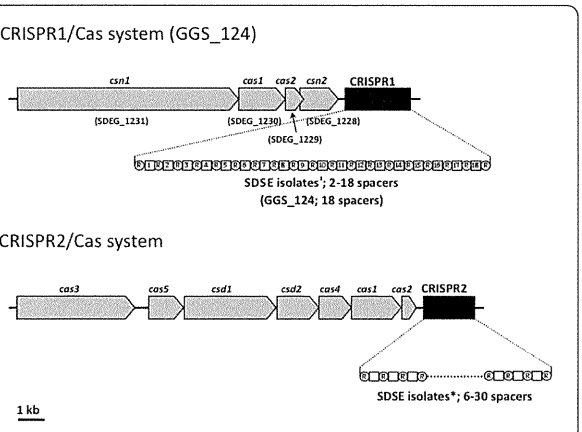

Figure 5 CRISPR/Cas system structures found in SDSE isolates. The CRISPR structures of SDSE isolates were analyzed by direct sequencing of PCR-amplified CRISPR regions. The repeat-spacer regions (CRISPR) are enlarged. Open circles marked "R" are direct repeats, whereas the square boxes indicate respective spacers with numbers. GGS_124 contained only CRISPR1, whereas some of the other strains also contained CRISPR2 (Table 2).

genes for mitogenic exotoxin Z (*smeZ*), which are present in GAS [37], were not found in the GGS_124 genome.

(iii) Proteases

We found that a putative proteinase (SDEG_1906) and streptococcal C5a peptidase (*scpB*) (SDEG_0933) [38] were conserved among GGS_124 and 5 closely related species. GGS_124 also has a gene with homology (42% amino acid identity) to exfoliative toxin A of *Staphylococcus aureus* strain Mu50 (SAV1173), which causes staphylococcal scalded skin syndrome [39]. GGS_124 also carries a gene for streptokinase (SDEG_0233), similar to streptokinase A of GAS, with 88% amino acid identity (Additional file 6). This protein complexes with plasminogen to form an activator, which has serine protease activity and cleaves free plasminogen. leading to activation of the zymogen [40]. Strikingly, GGS_124 lacks streptococcal cysteine protease (SpeB), an erythrogenic toxin produced by GAS with cysteine protease activity [41]. The GGS_124 genome lacks approximately 7 kb of

Table 2 Presence of Cas genes and the number of spacers in CRISPR1/Cas and CRISPR2/Cas

		CRISPR1/Cas			CRISPR2/Cas		
Species	**Strain**	**Cas genes**	**No. of spacers**	**Acc. No.**	**Cas genes**	**No. of spacers**	**Acc. No**
Streptococcus dysgalactiae subsp. *equisimilis*	GGS_124	+	18	AP010935.1	-	0	-
	168	+	2	AB553332	+	13	AB553333
	GGS_117	+	8	AB553338	+	12	AB553339
	170	+	9	AB553336	+	10	AB553337
	164	+	17	AB553343	+	6	AB553331
	GGS_118	+	8	AB553342	+	13	AB553341
	169	+	7	AB553334	+	30	AB553335
	163	+	3	AB553340	N. D.	N. D.	
Streptococcus pyogenes	MGAS8232	-	0	AE009949.1	-	0	0AE009949.1
	MGAS10394	-	0	CP000003.1	-	0	CP000003.1
	MGAS10750	+	0	CP000262.1	+	5	CP000262.1
	Manfredo	-	0	AM295007.1	-	0	AM295007.1
	MGAS10270	+	2	CP000260.1	+	3	CP000260.1
	MGAS315	+	0	AE014074.1	-	0	AE014074.1
	MGAS5005	+	3	CP000017.1	+	4	CP000017.1
	MGAS9429	+	0	CP000259.1	+	7	CP000259.1
	MGAS2096	+	0	CP000261.1	+	6	CP000261.1
	SF370	+	6	AE004092.1	+	3	AE004092.1
	SSI-1	+	0	BA000034.2	-	0	BA000034.2
	MGAS6180	+	4	CP000056.1	+	1	CP000056.1
	NZ131	+	4	CP000829.1	+	5	CP000829.1
Streptococcus equi subsp. *zooepidemicus*	MGCS10565	+	17	CP001129.1	+	9	CP001129.1
	H70	-	0	FM204884.1	+	18	FM204884.1
Streptococcus equi subsp. *equi*	4047	-	0	FM204883.1	-	0	FM204883.1

N.D.: No amplicon was obtained in PCR analyses.

the GAS strain MGAS315 sequence, including genes encoding SpeB (SpyM3_1742), the transcriptional regulator RopB (SpyM3_1744), and mitogenic factor 25K precursor (SpyM3_1745). Since several transposase and related genes (SDEG_0212, 0206, 0205, 0201, 0194) are located in the corresponding region, it is highly likely that the region that included *speB* was present in the common ancestor of GAS and SDSE but was not retained by SDSE after speciation.

We found that *speB* was not present in GGS_124, in agreement with the results of a microarray study, which showed that all of the 58 examined strains of group C and G SDSE isolated from patients lacked the *speB* gene [31,32]. We therefore examined whether SDSE strains have protease activity similar to that of SpeB (Additional file 7). We did not detect any SpeB-like protease activity in strains GGS_124 or GGS_118, which had been isolated from two patients with STSS. In contrast, a GAS strain produced a proteinase that was sensitive to E-64, which inhibits cysteine proteases, including SpeB.

(iv) FCT-like regions

Recently, GAS and GBS were shown to express pili, which are synthesized by proteins encoded by genes in FCT regions [1,42,43]. GGS_124 harbors 2 FCT-like regions, which are probable operons expressing different pilus-like structures (Figure 6). One of these contains genes encoding the transcriptional regulator RofA (SDEG_0156), two putative fimbrial structural subunit proteins (SDEG_0157 and SDEG_0158), two sortases (SDEG_0159 and SDEG_0160), and a putative fibronectin binding protein (SDEG_0161). It is similar to the FCT-6 region, which is conserved among M2 GAS, GBS, and SESZ [22,42,44]. The second region contains genes encoding a putative transcriptional regulator (SDEG_1782), a defective collagen binding protein (SDEG_1781), a signal peptidase I (SDEG_1780), a backbone protein (SDEG_1779), and an ancillary protein (SDEG_1778). It is similar to the FCT-3 region, which was found in M3, M5, M18, and M49 GAS [43].

(v) Adhesins

GGS_124 possesses genes that encode putative adhesion proteins, including proteins similar to putative fibronectin binding proteins (SDEG_0161, 1263, and 1984), pullulanase (SDEG_0237), phosphopyruvate hydratase (SDEG_0704), laminin binding protein (SDEG_0935), internalin protein (SDEG_1372), and collagen binding protein (SDEG_1781), all of which bind to the extracellular matrix (Additional file 6). SGGS_124 also possesses genes encoding immunoglobulin G binding protein (SDEG_1358) [45] and multifunctional streptococcal plasmin receptor (Plr)/streptococcal surface dehydrogenase (SDH)/glyceraldehyde-3-phosphate dehydrogenase (GAPDH), which binds to complement component C5a (SDEG_1936) [46] (Additional file 6), although the product of SDEG_1936 lacks a signal peptide.

(vi) Hyaluronan capsule synthesis

Hyaluronic acid (HA), synthesized *via* the *hasABC* operon, is considered a pleiotropic virulence factor involved in

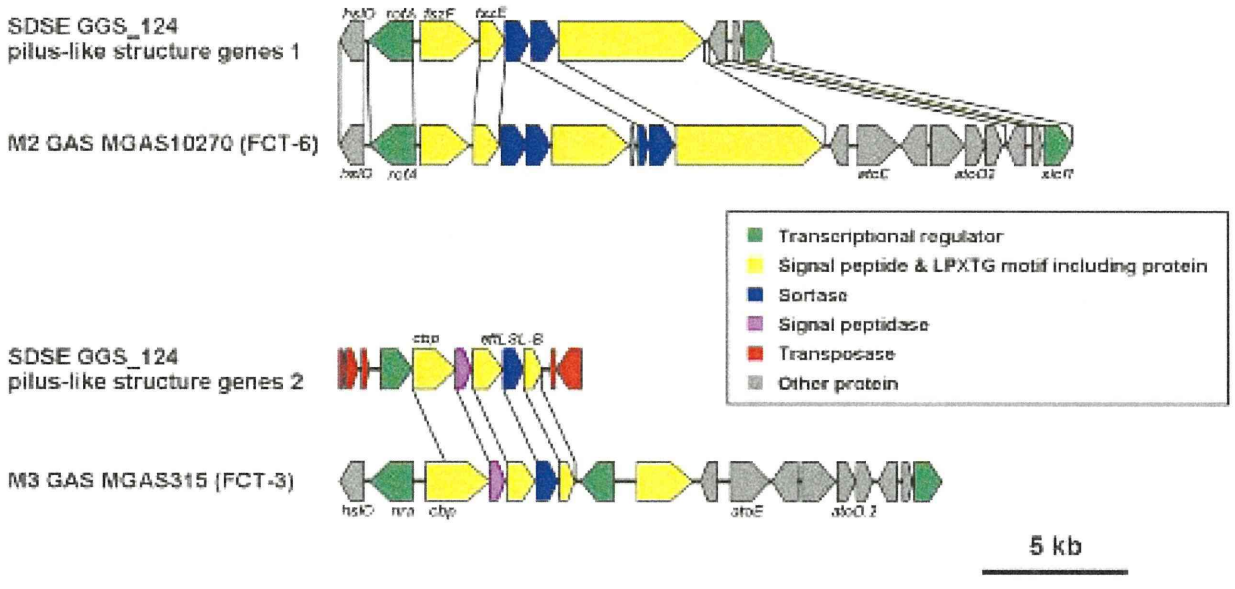

Figure 6 Organization of genes encoding pilus-like structure proteins in *S. dysgalactiae* subsp. *equisimilis* GGS_124. The organizations of genes encoding pilus-like structure proteins in GGS_124 were compared with those in GAS and SESZ. Colored boxes between genes indicate similarity at the amino acid level (red, ≥90%; orange, 90%-80%; yellow-green, 79%-70%; green, 69%-60%; purple, 59%-40%; gray, <40%).

many aspects of GAS infection [47]. GGS_124, however, does not contain an *hasABC* operon, in contrast to the genomes of GAS, SESZ, SESE, and *S. uberis*. Rather, GGS_124 possesses only one gene, encoding glycosyl transferase (SDEG_0628), which shows a low level of similarity to *hasA* of GAS (20% amino acid similarity). Although one SDSE strain has been shown to possess a hyaluronan synthase (AF023876.1), very similar to the product of *hasA* [48], GAS gene microarray analysis of 58 SDSE strains isolated from human infections showed that all harbored only hasC [31]. We found that GGS_124 also harbors only *hasC* (SDEG_1980) (Additional file 6), making it unlikely that SDSE produces HA *via* the *hasABC* operon.

(vii) Hyaluronidase

GGS_124 possesses a gene in a non-prophage region of the genome that encodes a putative hyaluronidase (SDEG_0654), with 66% identity to *hylB* in SESZ (Additional file 6). Hyaluronidase in GAS is thought to contribute to the spread of bacteria in tissues and may allow GAS to utilize host hyaluronic acid or its own capsule as an energy source [49]. The hyaluronidase in GGS_124 may have a function similar to that in GAS.

(viii) Nucleases

GGS_124 possesses 5 genes that encode putative nucleases with a secretion signal peptide: genome-encoded streptodornase (SDEG_0541), extracellular nuclease (SDEG_0714), DNA-entry nuclease (SDEG_0732), cell surface 5'-nucleotidase (SDEG_0825), and prophage-associated deoxyribonuclease (SDEG_1103), all of which are predicted to code for a secretion signal peptide. Two of them, SDEG_0714 and SDEG_0825, code for potential cell wall anchor motifs, LPKAG and LPMAG, respectively (Additional file 6). The putative streptodornase SDEG_0541 and DNA-entry nuclease SDEG_0732 are homologous to phage-encoded extracellular streptodornase D Sda1 of GAS (PHA01790) [50] and DNA-entry nuclease EndA of *S. pneumoniae* TIGR4 (SP_1964) [51], respectively (Additional file 6). Sda1 and EndA have been found to degrade neutrophil extracellular traps (NETs) [50,51], which are composed of granule proteins and chromatin released by neutrophils and can catch and kill surrounding bacteria [52]. The putative extracellular DNase SDEG_0714 is similar to M1 GAS cell-wall-located DNase SpnA (Spy0747), which has been reported important for virulence, *e.g.*, dispersion in host tissue [53] (Additional file 6).

(ix) Other virulence factors

GGS_124 possesses genes encoding the multifunctional M protein (*stg480.0*) (SDEG_0230). The M protein of GAS shows antiphagocytic and adhesin activities, whereas the adhesion function of the GGS M protein may be due to a collagen binding motif [54,55]. Since the product of *Stg480.0* lacks this motif, the M protein of GGS_124 may not act as an adhesin.

Streptococcal inhibitor of complement (SIC) and distantly related to SIC (DRS) are some extent of homology. DRS binds complement factors but does not inhibit complement mediated cell lysis [56,57], whereas SIC inhibits complement mediated cell lysis [58]. GGS_124 harbors a putative DRS gene (SDEG_0932), which consists of a signal sequence, two repeat regions, and a proline-rich region typical of DRS, and is homologous to the Drs12.04 protein of GAS strain *emm12* with 48% amino acid identity [59] (Additional file 6).

The GGS_124 genome harbors a gene encoding a collagen-like protein (SDEG_1113), similar to the collagen-like repeat phage protein of SESE 4047 (SEQ_0837), with 41% amino acid identity. Streptococcal collagen-like proteins (Scl) are cell-surface molecules of GAS with domains containing tracks of repeated Gly-Xaa-Yaa sequences that form a mammalian collagen-like triple-helical structure. These proteins mediate the internalization of GAS into human cells upon binding of Scl to the human collagen receptor integrin [60]. The GGS_124 gene encoding collagen-like protein does not contain a signal peptide or LPXTG motif, suggesting that the gene product may not be expressed on the cell surface. In contrast, GGS_124 does not harbor genes encoding proteins similar to the other collagen-like proteins (*sclA* and *sclB*) in GAS.

NAD glycohydrolase (SDEG_2029), which is located in the NADase-streptolysin O operon of the GAS genome [61], was found to be conserved in the same operon in GGS_124 (Additional file 6). This enzyme is expressed after streptolysin O is injected into host cells and accelerates cell death [61,62].

(x) Distribution of virulence factors among Streptococci

We also assessed the presence or absence of representative virulence factors among sequenced streptococcal species, including GAS (MGAS315), SESE (4047), SESZ (MGCS10565), GBS (A909), and *S. uberis* (0140J) (Additional file 8). Among 30 virulence factors, most of those located in the core genome, but not those located in streptococcal phages, are conserved in GGS_124, except for *speB*. In contrast, other *streptococci* lack genes encoding streptolysin O, NAD glycohydrolase and DRS (or SIC), suggesting the importance of these proteins in the pathogenicity of SDSE and GAS in humans, causing STSS.

Putative virulence factors unique to SDSE

We identified 20 gene products in GGS_124 containing signal peptides and LPXTG cell wall surface anchor motifs that showed low similarity to known proteins. Using PCR, we analyzed the distributions of these putative virulence factors in 8 SDSE isolates (Table 3 arranged according to their decreasing lethality in mice). A putative T-antigen-like protein structural subunit